

Electromagnetic pion and kaon form factors in light-cone resummed perturbative QCD

Udit Raha* and Andreas Aste†

Department of Physics, University of Basel, Switzerland

(Received 11 December 2008; published 18 February 2009)

We analyze the electromagnetic pion and kaon form factor by including radiative and higher-twist effects within the framework of resummed perturbative QCD in the spacelike region. We focus on the transition from the perturbative to nonperturbative behavior in the phenomenological intermediate-energy regime. Using a modified “ k_T ” factorization scheme with transverse degrees of freedom, we evaluate the nonperturbative soft contributions as distinct from the hard contributions, ensuring no double counting via the Ward identity at $Q^2 = 0$. The soft contributions are obtained via local quark-hadron duality, while the hard contributions rest on the well-known collinear factorization theorem using model wave functions with modified Brodsky-Huang-Lepage-type ansatz and distribution amplitudes derived from light-cone QCD sum rules. Our analysis shows that the perturbative hard part prevails for large Q^2 beyond 50–100 GeV², while for low and moderate momentum transfers below 10–16 GeV², the soft contributions dominate over the hard part. Thus, we demonstrate the importance of including the soft contributions for explaining the experimental form-factor data.

DOI: 10.1103/PhysRevD.79.034015

PACS numbers: 12.38.Bx, 12.38.Cy, 12.39.St, 13.40.Gp

I. INTRODUCTION

During the past decade, QCD-oriented studies have been shifting steadily toward exclusive channels. For a long time the electromagnetic structure of pions has been subjected to numerous experimental and theoretical investigations through the study of electroproduction reactions. Extensive experimental studies of pion electroproduction reactions like $ep \rightarrow e\pi^+n$ or $en \rightarrow e\pi^-p$ have been carried out in the past at CERN, Cornell, DESY, and, more recently, at JLab [1–8]. Since the mid-1990s, kaon electroproduction reactions like $A(\gamma, K)YB$ and $A(e, e'K)YB$ (A is the target, Y the produced hyperon, and B the recoil) have also attracted renewed interest in nuclear physics at both experimental [9,10] and theoretical [11,12] levels. The main ingredients for the description of electromagnetically induced kaon production are embedded in the so-called Chew, Goldberger, Low, and Nambu (CGLN) scattering amplitudes. In the case of the longitudinal component of the electron induced unpolarized differential cross section, the t -channel diagram dominates and (in certain kinematic conditions) can be factorized [9,13] as $\sigma_L = k \cdot \mathcal{F}(Q^2)\mathcal{G}(W)\mathcal{H}(t)$, where k is a kinematic factor, and \mathcal{F} , \mathcal{G} , and \mathcal{H} are functions of the 4-momentum transfer squared Q^2 of the virtual photon, the invariant mass W , and the Mandelstam variable t , respectively. The function $\mathcal{F}(Q^2)$ implicitly contains the information about the electromagnetic form factor of the kaon. Note that $\mathcal{F}(Q^2)$ is not the actual form factor, but rather a complicated function from which the form factor can be extracted using, e.g., Chew-Low extrapolation and deconvolution algorithms. A precise knowledge of the form factor is of

fundamental importance for a realistic and accurate description of *exclusive reaction* mechanisms, and it plays a key role in understanding the interplay between perturbative and nonperturbative physics at intermediate energies. Moreover, the study of form factors provides direct insight into the electromagnetic structures and charge distributions of hadrons as they couple with photons.

To date, the electromagnetic kaon form factor is very poorly known and only measured at very low Q^2 (below 0.2 GeV²) [14,15]. The status for the (quasifree) Lambda (Λ) and Sigma (Σ) hyperons is even worse; i.e., there are simply no available experimental data. Basic quantities like the strong coupling constants $g_{K\Lambda N}$ and $g_{K\Sigma N}$ derived from purely hadronic processes or theoretical considerations are not well established and must be considered adjustable. Recently, however, there appeared quite large and precise data sets on photo-production of kaons from the SAPHIR (ELSA) [16], CLAS (CEBAF) [17], and LEPS (SPRING8) [18] collaborations. There is also new data on electroproduction of positive kaons from experiment E98-108 at CEBAF which are being analyzed at the moment.

Keeping in mind the increasing accuracy of experimental data, an accurate theoretical description of the electromagnetic form factors of pseudoscalar charged mesons at intermediate energies is of primal importance. To our knowledge, especially for the kaon, there are very few theoretical works in this direction [19–22]. In this paper, in addition to the pion form factor, we analyze the kaon form factor for a broad range of spacelike momentum transfers. Our framework is based on resummed perturbative light-cone QCD formalism [23,24], unlike conventional approaches like “asymptotic” and lattice QCD or from sum rules that rely on many unchecked hypotheses. The experimental results could then be used to extract the

*Udit.Raha@unibas.ch

†Andreas.Aste@unibas.ch

various *distribution amplitudes* (DAs) [25–42] used in the above formulation. Of course, only a handful of experimental hadron electroproduction data points are presently available to make definitive statements on the validity of different theoretical approaches. Since in almost all cases the corresponding data points are merely concentrated in the very low-energy region ($Q^2 < 1 \text{ GeV}^2$), perturbative QCD (pQCD) has limited predictive power due to the rapidly growing magnitude of the strong coupling, as Q^2 tends to zero. Despite the existing plethora of literature on the predictions of electromagnetic meson form factors based on various approaches (see e.g., Refs. [22–24,40–73] for the pion and Refs. [19–22] for kaon form factors, to give a highly incomplete list of references), to date there is a considerable amount of debate as to their exact behavior in the phenomenological low and moderate energies in the range $Q^2 \approx 4\text{--}50 \text{ GeV}^2$. Nevertheless, we try to give our assessment to the existing scenario and try to explain the experimental data first for the pion form factor, where statistics are far more decent as compared to that of the kaon. Then we extend our analysis to the kaon form factor, where experimental data are still too limited for any meaningful comparison. Hopefully, with the planned 12 GeV upgrade proposal of the CEBAF experiment (at JLab) in the near future, studies of intermediate-energy QCD can prove to be fruitful.

The standard asymptotic QCD is known to make successful predictions of many phenomena like *dimensional scaling*, *helicities*, *color transparency*, etc. for exclusive processes, as Q^2 tends to infinity [48,71–74]. The approach relies on the so-called *collinear factorization* theorem [72,73] which provides an outstanding way of isolating the partonic part accessible to pQCD from the nonperturbative parts. The basic ingredients are as follows: (a) the hadron DA ϕ , which encodes the nonperturbative information regarding the momentum distribution of the constituent “near” on-shell valence partons collinear to the hadron and also features of the QCD vacuum structure as expressed through the quark condensates [75–77], and (b) a scattering kernel T_H , describing the hard scattering of “far” off-shell valence partons. The overall amplitude of the exclusive process is then given by the convolution $\phi \otimes T_H \otimes \phi$. However, the application of pQCD to exclusive processes at intermediate momentum transfers or phenomenologically accessible energies (e.g., at CEBAF) has been the subject of severe controversies and criticisms [70,78–86]. It is widely anticipated that nonperturbative effects arising from soft gluon exchanges or from endpoint contributions to phenomenologically acceptable wave functions (or DAs) dominate and may severely preclude the predictability of pQCD. Hence, in this paper we use a modified “resummed” pQCD formalism (as proposed in Refs. [23,24]) which is believed to largely enhance the predictability of pQCD in a self-consistent way at intermediate energies. The central issue here is the inclusion of

transverse momentum k_T dependence that necessitates the inclusion of a *Sudakov suppression* factor. The purpose of this Sudakov factor is to organize the large double logarithms of the type $\alpha_s \ln^2 k_T$, arising at all orders due to the overlap of soft and collinear contributions of radiative gluon loop corrections. Such a resummation effectively suppresses the nonperturbative contributions at large energies. However, this still may not be effective enough when we talk about Q^2 down to a few GeV^2 . These facts are in agreement with some of the recent findings, reported in Refs. [63–65] for the pion form factor, and also in the context of B systems [87].

In this paper, we emphasize the importance of including two distinct contributions to exclusive quantities for obtaining good agreement with experimental data at low and moderate energies: first, the nonfactorizable soft contributions which are not calculable within the perturbative framework, and second, the power suppressed corrections from nonleading twist structures (twist-3) determining the preasymptotic behavior. In other words, the electromagnetic form factor $F_M(Q^2)$ for a charged meson M should be written as

$$F_M(Q^2) = F_M^{\text{soft}}(Q^2) + F_M^{\text{hard}}(Q^2), \quad (1)$$

where $F_M^{\text{hard}}(Q^2)$ is the factorizable part computable in pQCD and $F_M^{\text{soft}}(Q^2)$ is the nonfactorizable soft part. The soft contributions to the form factors can be calculated using phenomenological quark models, either incorporating transverse structure (momentum) dependence of the hadron wave functions (see, e.g., Refs. [61,79,81,82,88]) or from QCD sum rules via *local duality* (see, e.g., Refs. [49–52,62,89]). In the present paper, we follow the latter approach. We also focus on the presence of nonperturbative enhancements arising from kinematic endpoint regions of the scattering kernel which tend to invalidate collinear factorization. For our calculations, we use model twist-2 and twist-3 light-cone wave functions incorporating transverse degrees of freedom, where the collinear DAs are derived from QCD sum rules [35–39]. Naively, the twist-3 contributions to the form factor are expected to be small compared to leading (twist-2) contributions, as they have a relative $1/Q^2$ suppression. On the contrary, the existing literature, either using model or asymptotic DAs [26,28,29,58,63,65], shows large twist-3 corrections to the pion form factor which even overshoot the twist-2 contributions in a wide range of low and intermediate energies. This is also confirmed in our analysis and is in fact more enhanced for the kaon form factor. To this end, our analysis shows good agreement with the existing pion data, and in addition we prove the consistency of our results by adopting a scheme of analytization of the running strong coupling [61,62,90,91] that removes the explicit Landau singularity at $Q^2 = \Lambda_{\text{QCD}}^2$ by a minimum power correction in the UV regime.

The paper is organized as follows: In Sec. II, we briefly discuss the idea of factorization and review the basic definitions of the twist-2 and twist-3 pseudoscalar meson DAs and their renormalization evolutions. Section III deals with the theoretical framework involved in calculating the spacelike electromagnetic form factor. Here, we recall the predictions of classic asymptotic QCD for large $Q^2 \rightarrow \infty$ and how one needs to modify pQCD with collinear as well as “ k_T ” factorization schemes, including Sudakov effects at intermediate energies. In Sec. IV, we provide the details of our numerical results for the pion form factor and compare them with the available experimental data. We also give a preliminary prediction for the kaon form factor, despite the lack of available experimental data for comparison in the desired phenomenological regime. Finally, Sec. V contains our summary and conclusions. The appendixes contain a compendium of relevant formulas used in our analysis.

II. FACTORIZATION AND DISTRIBUTION AMPLITUDES

The parton model of describing exclusive processes in QCD inherently rests on the so-called *frozen approximation* [71–73]. At high energies, exclusive scattering amplitudes are dominated by hadronic Fock states with essentially valence quark configurations ($\bar{q}q$ in mesons). While the relative velocities of the participating hadrons are located close to the null plane, the internal hadron “-quantum-binding” processes are highly time-dilated with respect to the exclusive reaction time scales in the rest frames of the remaining hadrons. This effectively freezes the hadronic internal degrees of freedom as seen by the other hadrons. This incoherence between the long-distance intrahadronic binding processes and the short-distance interhadronic scattering reaction is the very motivation for the idea of factorization. Thus, the hadrons may be considered to be consisting of definite valence quark states denoted by a DA of leading twist ϕ . The collinear factorization formula is then used to express exclusive quantities like the form factors as a convolution using the DAs:

$$F_M(Q^2) = \int_0^1 dx dy \phi_{\text{in}}(x, \mu_F^2) T_H(x, y, Q^2, \mu_F^2, \mu_R^2) \times \phi_{\text{out}}(y, \mu_F^2) + \dots, \quad (2)$$

where $Q^2 = -2P_{\text{in}} \cdot P_{\text{out}}$. Here, P_{in} and P_{out} are, respectively, the ingoing and outgoing hadron momenta, x and y are the longitudinal momentum fractions of the nearly on-shell valence quarks, μ_R is the renormalization scale, and μ_F is the factorization scale which is defined as the scale below which the QCD dynamics are nonperturbative and remain implicitly encoded within the DAs, while the dynamics above are perturbative and must be retained in the hard kernel T_H . The ellipses in the above equation represent contributions from higher order Fock states and sub-leading twists which are all suppressed by inverse powers

of Q^2 . In addition, they also include the nonfactorizable soft contributions. Formally, the definition of the leading twist-2 DA for pseudoscalar mesons (e.g., π^-) can be given in a process- and frame-independent manner [35,36,71–73] in terms of matrix elements of a nonlocal light-ray operator along a certain lightlike direction $z_\mu (z^2 = 0)$:

$$\langle 0 | \bar{u}(z) [z, -z] \gamma_\mu \gamma_5 d(-z) | \pi^-(P) \rangle = iP_\mu \int_0^1 dx e^{i\xi(z \cdot P)} \phi_{2;\pi}(x, \mu_F^2); \quad \xi = 2x - 1, \quad (3)$$

with the path-ordering (\mathcal{P}) Wilson line in terms of the gluon “connection” along the straight line joining z and $-z$ along the null plane which is given by

$$[z, -z] = \mathcal{P} \left[ig_s \int_{-z}^z dy^\mu A_\mu(y) \right], \quad (4)$$

where $P_\mu^2 = m_\pi^2$ and p_μ is a lightlike vector,

$$p_\mu = P_\mu - \frac{1}{2} z_\mu \frac{m_\pi^2}{P_z}. \quad (5)$$

The local limit $z \rightarrow 0$ gives the normalization condition at an arbitrary scale μ ,

$$\int_0^1 \phi_{2;\pi}(x, \mu^2) dx = \frac{f_\pi}{2\sqrt{2N_c}} \quad (6)$$

with the pion decay constant, $f_\pi \approx 131$ MeV, defined by

$$\langle 0 | \bar{u}(0) \gamma_\mu \gamma_5 d(0) | \pi^-(P) \rangle = if_\pi P_\mu. \quad (7)$$

The leading twist-2 DA $\phi_{2;\pi}(x, \mu^2)$ can be expressed as a conformal series expansion over Gegenbauer polynomials $C_{2n}^{3/2}$:

$$\phi_{2;\pi}(x, \mu^2) = \frac{3f_\pi}{\sqrt{2N_c}} x(1-x) \left(1 + \sum_{n=1}^{\infty} a_{2n}^\pi(\mu^2) C_{2n}^{3/2}(\xi) \right), \quad (8)$$

where

$$\phi_{2;\pi}^{(\text{as})}(x) = \phi_{2;\pi}(x, \mu^2 \rightarrow \infty) = \frac{3f_\pi}{\sqrt{2N_c}} x(1-x) \quad (9)$$

is generally referred to as the *asymptotic* DA. The Gegenbauer moments a_{2n}^π represent the nonperturbative inputs encoding the long-distance dynamics and may be obtained, e.g., via lattice QCD calculations or QCD sum rules. The renormalization group (RG) equation for $\phi_{2;\pi}(x, \mu^2)$ is known as the Efremov-Radyushkin-Brodsky-Lepage (ER-BL) equation [71–73],

$$\mu^2 \frac{d}{d\mu^2} \phi_{2;\pi}(x, \mu^2) = \int_0^1 dy V(x, y; \alpha_s(\mu^2)) \phi_{2;\pi}(y, \mu^2) \quad (10)$$

with the integral kernel $V(x, y; \alpha_s)$ to leading order in α_s given by

$$V_0(x, y; \alpha_s) = C_F \frac{\alpha_s}{2\pi} \left[\frac{1-x}{1-y} \left(1 + \frac{1}{x-y} \right) \theta(x-y) + \frac{x}{y} \left(1 + \frac{1}{y-x} \right) \theta(y-x) \right]_+, \quad (11)$$

where the “+” distribution is defined as

$$[V(x, y; \alpha_s)]_+ = V(x, y; \alpha_s) - \delta(x-y) \int_0^1 dt V(t, y; \alpha_s). \quad (12)$$

Solving the above set of equations yields the multiplicative renormalization formula for moments a_n^π to leading-logarithmic accuracy,

$$a_n(\mu^2) = L^{\gamma_n^{(0)}/\beta_0} a_n(\mu_0^2), \quad (13)$$

where $L = \alpha_s(\mu^2)/\alpha_s(\mu_0^2)$ and $\beta_0 = (11N_c - 2N_f)/12$, while the lowest order anomalous dimensions are given by

$$\gamma_n^{(0)} = C_F \left(\psi(n+2) + \psi(1) - \frac{3}{4} - \frac{1}{2(n+1)(n+2)} \right) \quad (14)$$

with the logarithmic derivative of the Gamma function $\psi(z) = \Gamma'(z)/\Gamma(z)$. Note that for the pion all odd moments $a_{n=1,3,5,\dots}^\pi$ vanish due to isospin symmetry. In contrast, the kaon DAs have nonzero values for the odd moments, signifying flavor-SU(3) violation effects. Hence, the twist-2 DA for the kaon (e.g., K^-) is given by the expansion

$$\phi_{2,K}(x, \mu^2) = \frac{3f_K}{\sqrt{2N_c}} x(1-x) \left(1 + \sum_{n=1}^{\infty} a_n^K(\mu^2) C_n^{3/2}(\xi) \right), \quad (15)$$

$$\int_0^1 \phi_{2,K}(x, \mu^2) dx = \frac{f_K}{2\sqrt{2N_c}}, \quad (16)$$

where the kaon decay constant $f_K \approx 1.22f_\pi$ [25] is defined by

$$\langle 0 | \bar{u}(0) \gamma_\mu \gamma_5 s(0) | K^-(P) \rangle = i f_K P_\mu. \quad (17)$$

Since the Gegenbauer moments are multiplicatively renormalizable with growing anomalous dimensions, for a sufficiently large renormalization scale a finite number of moments are relevant, despite the fact that the higher order moments have large uncertainties in their present determination. Hence, in all practical calculations, the series expansions of the DAs are truncated only to the first few moments. In this paper, we have adopted a model for the twist-2 DAs in truncating up to the second moment, as was done in Refs. [36,38].

For the charged pseudoscalar mesons at the twist-3 level, there are two 2-particle DAs and one 3-particle DA. Here, we only give the formal definitions of the 2-particle DAs that we need in our analysis. For the charged pion (e.g.,

π^-), they are defined by [35]

$$\begin{aligned} \langle 0 | \bar{u}(z) i \gamma_5 d(-z) | \pi^-(P) \rangle &= \mu_\pi \int_0^1 dx e^{i\xi(zp)} \phi_{3;\pi}^p(x, \mu^2), \\ \langle 0 | \bar{u}(z) \sigma_{\alpha\beta} \gamma_5 d(-z) | \pi^-(P) \rangle &= -\frac{i}{3} \mu_\pi (P_\alpha z_\beta - P_\beta z_\alpha) \\ &\quad \times \int_0^1 dx e^{i\xi(zp)} \phi_{3;\pi}^\sigma(x, \mu^2) \end{aligned} \quad (18)$$

with $\mu_\pi = m_\pi^2/(m_u + m_d)$ and similarly for the charged kaon (e.g., K^-) [38]:

$$\begin{aligned} \langle 0 | \bar{u}(z) i \gamma_5 s(-z) | K^-(P) \rangle &= \mu_K \int_0^1 dx e^{i\xi(zp)} \phi_{3;K}^p(x, \mu^2), \\ \langle 0 | \bar{u}(z) \sigma_{\alpha\beta} \gamma_5 s(-z) | K^-(P) \rangle &= -\frac{i}{3} \mu_K (P_\alpha z_\beta - P_\beta z_\alpha) \\ &\quad \times \int_0^1 dx e^{i\xi(zp)} \phi_{3;K}^\sigma(x, \mu^2) \end{aligned} \quad (19)$$

with $\mu_K = m_K^2/(m_u + m_s)$. Note that the gauge-link factors [Wilson line (4)] in the matrix elements are to be implicitly understood. The twist-3 DAs have the following asymptotic forms:

$$\begin{aligned} \phi_{3;M}^{p(\text{as})}(x) &= \frac{f_M}{4\sqrt{2N_c}}, & \phi_{3;M}^{\sigma(\text{as})}(x) &= \frac{3f_M}{2\sqrt{2N_c}} x(1-x); \\ M &= \pi^\pm, K^\pm \end{aligned} \quad (20)$$

with the normalization condition

$$\int_0^1 \phi_{3;M}^{p,\sigma}(x, \mu^2) = \frac{f_M}{4\sqrt{2N_c}}. \quad (21)$$

For our analysis, we use the 2-particle twist-3 DAs from Refs. [36,38] defined at the scale $\mu = 1$ GeV. As a matter of bookkeeping, we explicitly provide the relevant formulas for the charged pion and kaon DAs in Appendix A.

III. SPACELIKE ELECTROMAGNETIC FORM FACTOR

The electromagnetic form factor is considered an important observable for studying the onset of the perturbative regime in exclusive processes. For large Q^2 , the asymptotic scaling behavior $F_M(Q^2) \sim 1/Q^2$ follows from the well-known dimensional “quark counting,” while for small Q^2 , the behavior is well described by the vector meson dominance (VMD) model [43–45] and is given by

$$F_M(Q^2) \approx \frac{1}{1 + Q^2/\mu_{\text{VDM}}^2}; \quad Q^2 \ll \mu_{\text{VDM}}^2, \quad (22)$$

where $\mu_{\text{VDM}} \approx 750$ MeV is a reasonable cutoff mass scale, showing no obvious trace of pQCD scaling behavior where no high-energy cutoff exists. Hence, a thorough understanding of this transition (from nonperturbative to

perturbative) behavior is of crucial importance in QCD for understanding the very nature of strong interactions and in providing a vivid picture of the underlying quark-gluon substructure of the mesons.

For a charged meson M (e.g., π^\pm , K^\pm), the form factor is specified by the following matrix element:

$$(P' + P)_\mu F_M(Q^2) = \langle M(P') | J_\mu(0) | M(P) \rangle; \quad (23)$$

$$J_\mu = \sum_f e_f \bar{q}_f \gamma_\mu q_f,$$

where J_μ is the electromagnetic current with quark q_f of flavor f and charge e_f . In this paper, we shall only consider spacelike momentum transfers, i.e., $q^2 = (P' - P)^2 = -Q^2$. Neglecting the meson masses, we consider the ‘‘brick wall’’ frame where the incoming particle with 4-momentum P in the z direction recoils with 4-momentum P' in the $-z$ direction after interacting with the hard photon ‘‘wall.’’ In the light-cone formalism, $P = (Q/\sqrt{2}, \mathbf{0}_T)$ and $P' = (0, Q/\sqrt{2}, \mathbf{0}_T)$.

A. Hard contributions in pQCD

The hard contributions to the form factor are calculated using the collinear factorization formula, Eq. (2), where the hard scattering kernel T_H at the scale $\mu = \mu_F = \mu_R$ is given to the leading order in α_s by

$$T_H(x, y, Q^2, \mu^2) = 16\pi C_F \alpha_s(\mu^2) \left[\frac{2}{3} \frac{1}{xyQ^2} + \frac{1}{3} \times \frac{1}{(1-x)(1-y)Q^2} \right], \quad (24)$$

where in QCD the value of the *Casimir* operator in the fundamental representation of SU(3) is $C_F = (N_c^2 - 1)/2N_c = 4/3$. The factorization formula then yields the classic pQCD expression for the meson form factor at $\mu^2 = Q^2$:

$$F_M^{\text{hard}}(Q^2) = \frac{16\pi C_F \alpha_s(Q^2)}{Q^2} \left| \int_0^1 dx \frac{\phi_{2:M}(x, Q^2)}{x} \right|^2. \quad (25)$$

$$\mathcal{P}_{2:M}(x_i, b_i, P_i \simeq Q, \mu) = \exp[-S_i(XQ, b_i, \mu)] \tilde{\mathcal{P}}_{2:M}(x_i, b_i, 1/b_i);$$

$$S_i(XQ, b_i, \mu) = s(x_i Q, 1/b_i) + s((1-x_i)Q, 1/b_i) + 2 \int_{1/b_i}^\mu \frac{d\bar{\mu}}{\bar{\mu}} \gamma_q(\alpha_s(\bar{\mu}^2)),$$

$$s(XQ, 1/b_i) = \int_{1/b_i}^{XQ/\sqrt{2}} \frac{d\mu}{\mu} \left[\ln\left(\frac{XQ}{\sqrt{2}\mu}\right) \mathcal{A}(\alpha_s(\mu^2)) + \mathcal{B}(\alpha_s(\mu^2)) \right], \quad (29)$$

where $1/b_1, 1/b_2$ set the factorization scales in the transverse impact configuration. In the above equations, the quark anomalous dimension is given by $\gamma_q(\alpha_s) = -\alpha_s/\pi$, and the ‘‘cusp’’ anomalous dimensions \mathcal{A} and \mathcal{B} , to one-loop accuracy, are given by

$$\mathcal{A}(\alpha_s(\mu^2)) = C_F \frac{\alpha_s(\mu^2)}{\pi} + \left[\left(\frac{67}{27} - \frac{\pi^2}{9} \right) N_c - \frac{10}{27} N_f + \frac{8}{3} \beta_0 \ln\left(\frac{e^{\gamma_E}}{2}\right) \right] \left(\frac{\alpha_s(\mu^2)}{\pi} \right)^2, \quad (30)$$

$$\mathcal{B}(\alpha_s(\mu^2)) = \frac{2}{3} \frac{\alpha_s(\mu^2)}{\pi} \ln\left(\frac{e^{2\gamma_E-1}}{2}\right)$$

Note that using the asymptotic twist-2 DA $\phi_{2:M}^{\text{(as)}}(x)$, one obtains the familiar $1/Q^2$ scaling behavior for $Q^2 \rightarrow \infty$,

$$F_M^{\text{hard}}(Q^2) = \frac{8\pi\alpha_s(Q^2)f_M^2}{Q^2}. \quad (26)$$

The principal motivation of the modified resummed pQCD is the elimination of large logarithms in the hard kernel that arise from radiative gluon loop corrections. One way of doing this is by the introduction of intrinsic transverse momenta dependence of the constituent partons, giving rise to a Sudakov suppression due to certain partial resummation of transverse terms, as mentioned earlier in the Introduction. Including the transverse momenta of the two valence quarks within the meson, the tree-level hard kernel T_H in momentum space is written as

$$T_H(x, y, Q^2, \mathbf{k}_{1T}, \mathbf{k}_{2T}, \mu^2) = \frac{16\pi C_F \alpha_s(\mu^2) x Q^2}{(xQ^2 + \mathbf{k}_{1T}^2)(xyQ^2 + (\mathbf{k}_{1T} - \mathbf{k}_{2T})^2)}, \quad (27)$$

where the transverse momentum dependence now sets the factorization scale. Then the modified factorization formula in the transverse *impact parameter* representation is given by

$$F_M^{\text{hard}}(Q^2) = \int_0^1 dx dy \int \frac{d^2 b_1}{(2\pi)^2} \frac{d^2 b_2}{(2\pi)^2} \mathcal{P}_{2:M}(x, b_1, P, \mu) \times \tilde{T}_H(x, y, Q, b_1, b_2, \mu) \mathcal{P}_{2:M}(y, b_2, P', \mu), \quad (28)$$

where the modified DA $\mathcal{P}_{2:M}(x_i, b_i, P_i, \mu)$ absorbs the large infrared logarithms into the Sudakov exponent S_i [23] (including also the evolution of the DA from the factorization scale $1/b_i$ to the scale μ):

where the $\overline{\text{MS}}$ running coupling to two-loop accuracy in standard perturbation theory is given by

$$\frac{\alpha_s(\mu^2)}{\pi} = \frac{1}{\beta_0 \ln(\mu^2/\Lambda_{\text{QCD}}^2)} - \frac{\beta_1 \ln(\ln(\mu^2/\Lambda_{\text{QCD}}^2))}{\beta_0^2 \ln^2(\mu^2/\Lambda_{\text{QCD}}^2)} \quad (31)$$

with $\beta_0 = (11N_c - 2N_f)/12 = 9/4$ and $\beta_1 = (51N_c - 19N_f)/24 = 4$ for $N_c = N_f = 3$. Note that the above-modified factorization calls for introducing a scale hierarchy $XQ > 1/b_i > \Lambda_{\text{QCD}}$ [where $X = x_i, (1 - x_i), x_1 = x$, and $x_2 = y$] to separate the distinct contributions from the perturbative and nonperturbative kinematic regions without the possibility of ‘‘double counting.’’ Note that there exist other schemes of defining the running coupling involving power corrections, restoring the explicit Landau singularity and the analyticity at $Q^2 = 0$ (see, e.g., Refs. [90,91] and also Sec. IV for details).

At low momentum transfers, the modified infrared-free DAs are often approximated with constituent quark masses which are different from the actual masses of the current quarks and usually chosen close to the intrinsic transverse scale Λ_{QCD} of the hadron structure, i.e., between 200 and 500 MeV. These quark masses, which effectively parametrize the QCD vacuum effects, are also used to suppress possible endpoint effects. Hence, we have

$$\tilde{\mathcal{P}}_{2:M}(x_i, b_i, 1/b_i) \simeq \tilde{\mathcal{P}}_{2:M}(x_i, b_i, 1/b_i, \mathcal{M}_q) \quad (32)$$

which could be expressed in terms of the full momentum-space light-cone wave function $\Psi_{2:M}$ (which also includes the transverse momentum distribution of the constituent bound state partons):

$$\begin{aligned} \tilde{\mathcal{P}}_{2:M}(x_i, b_i, 1/b_i, \mathcal{M}_q) \\ = \int_{\mathbf{k}_{iT}^2 \leq (1/b_i)^2} \frac{d^2 \mathbf{k}_{iT}}{16\pi^3} \Psi_{2:M}(x_i, \mathbf{k}_{iT}, 1/b_i, \mathcal{M}_q). \end{aligned} \quad (33)$$

To model the intrinsic transverse momentum dependence of the meson wave functions, we use the Brodsky-Huang-Lepage (BHL) Gaussian prescription [82,88]:

$$\Psi_{2:M}(x_i, \mathbf{k}_{iT}, 1/b_i, \mathcal{M}_q) = \Phi_{2:M}(x_i, 1/b_i) \Sigma(x_i, \mathbf{k}_{iT}, \mathcal{M}_q) \quad (34)$$

with

$$\Phi_{2:M}(x_i, 1/b_i) = A_{2:M} \phi_{2:M}(x_i, 1/b_i), \quad (35)$$

$$\Sigma(x_i, \mathbf{k}_{iT}, \mathcal{M}_q) = \frac{16\pi^2 \beta_{2:M}^2}{x_i(1-x_i)} \exp\left[-\frac{\beta_{2:M}^2}{x_i(1-x_i)} (\mathbf{k}_{iT}^2 + \mathcal{M}_q^2)\right], \quad (36)$$

assuming equal masses of the two constituent quarks within the meson. The parameters $A_{2:M}$, $\beta_{2:M}$, and \mathcal{M}_q are fixed using phenomenological constraints. The above

integration then yields the full modified wave function in the impact representation:

$$\begin{aligned} \tilde{\mathcal{P}}_{2:M}(x_i, b_i, 1/b_i, \mathcal{M}_q) &= A_{2:M} \phi_{2:M}(x_i, 1/b_i) \\ &\times \exp\left[-\frac{\beta_{2:M}^2 \mathcal{M}_q^2}{x_i(1-x_i)}\right] \\ &\times \exp\left[-\frac{b_i^2 x_i(1-x_i)}{4\beta_{2:M}^2}\right]. \end{aligned} \quad (37)$$

Including the RG evolution equation for the hard kernel,

$$\begin{aligned} \tilde{T}_H(x, y, Q, b_1, b_2, \mu) &= \exp\left[-4 \int_{\mu}^t \frac{d\bar{\mu}}{\bar{\mu}} \gamma_q(\alpha_s(\bar{\mu}^2))\right] \\ &\times \tilde{T}_H(x, y, Q, b_1, b_2, t), \end{aligned} \quad (38)$$

where

$$t = \max(\sqrt{xy}Q, 1/b_1, 1/b_2), \quad (39)$$

one arrives at the ‘‘double- b ’’ factorization formula for the meson form factor at the twist-2 level [59]:

$$\begin{aligned} F_M^{(t=2)}(Q^2) &= 16\pi Q^2 C_F \int_0^1 x dx dy \int_0^\infty b_1 db_1 b_2 db_2 \alpha_s(t) \\ &\times \tilde{\mathcal{P}}_{2:M}(x, b_1, 1/b_1, \mathcal{M}_q) \\ &\times \tilde{\mathcal{P}}_{2:M}(y, b_2, 1/b_2, \mathcal{M}_q) H(x, y, Q, b_1, b_2) \\ &\times \exp[-S(x, y, b_1, b_2, Q)] \end{aligned} \quad (40)$$

with

$$\begin{aligned} H(x, y, Q, b_1, b_2) &= K_0(\sqrt{xy}Qb_2) [\theta(b_1 - b_2) K_0(\sqrt{x}Qb_1) \\ &\times I_0(\sqrt{x}Qb_2) + \theta(b_2 - b_1) K_0(\sqrt{x}Qb_2) \\ &\times I_0(\sqrt{x}Qb_1)]. \end{aligned} \quad (41)$$

K_0 and I_0 are modified Bessel functions, and the full Sudakov exponent is given by

$$\begin{aligned} S(x, y, b_1, b_2, Q) &= \sum_{i=1}^2 \left[s(x_i Q, 1/b_i) + s((1-x_i)Q, 1/b_i) \right. \\ &\left. + 2 \int_{1/b_i}^t \frac{d\bar{\mu}}{\bar{\mu}} \gamma_q(\alpha_s(\bar{\mu}^2)) \right]. \end{aligned} \quad (42)$$

For completeness, the expression for the full Sudakov factor $s(XQ, 1/b_i)$, up to next-to-leading logarithm accuracy, is given in Appendix B. The expression slightly differs from the result given in Ref. [92], but numerically this difference is insignificant at our working accuracy. Note that this difference was first observed in Ref. [61].

To include the subleading twist-3 corrections to the form factor, the hard scattering kernel gets slightly modified as compared to the twist-2 case which turns out to be [58]

$$T_H^{(t=3)}(x, y, Q^2, \mathbf{k}_{1T}, \mathbf{k}_{2T}, \mu^2) = \frac{64\pi C_F \alpha_s(\mu^2) x}{(xQ^2 + \mathbf{k}_{1T}^2)(xyQ^2 + (\mathbf{k}_{1T} - \mathbf{k}_{2T})^2)}. \quad (43)$$

Applying the momentum projection operator [93,94]

$$\mathcal{M}_{\alpha\beta}^M = i \left\{ \not{n} \gamma_5 \Psi_{2,M} - \mu_M \gamma_5 \left(\Psi_{3,M}^p - i \sigma_{\mu\nu} n^\mu \bar{n}^\nu \frac{\Psi_{3,M}^{\sigma'}}{6} + i \sigma_{\mu\nu} P^\mu \frac{\Psi_{3,M}^\sigma}{6} \frac{\partial}{\partial k_{T\nu}} \right) \right\}_{\alpha\beta} \quad (44)$$

on the bilocal matrix element with quark flavors f_1 and f_2 ($f_{1,2} = u, d, s$),

$$\langle 0 | \bar{q}_{f_1}(z) q_{f_2}(-z) | M(P) \rangle_{\alpha\beta} = i \int_0^1 dx \int d^2 \mathbf{k}_T e^{i\xi(zp)} \left\{ \not{n} \gamma_5 \Psi_{2,M} - \mu_M \gamma_5 \left(\Psi_{3,M}^p - \sigma_{\mu\nu} P^\mu z^\nu \frac{\Psi_{3,M}^\sigma}{6} \right) \right\}_{\alpha\beta}, \quad (45)$$

where $\Psi_{3,M}^{\sigma'}(x, \mathbf{k}_T, 1/b, \mathcal{M}_q) = \partial \Psi_{3,M}^\sigma(x, \mathbf{k}_T, 1/b, \mathcal{M}_q) / \partial x$, $n = (1, 0, \mathbf{0}_T)$ is the unit vector in the “+” direction, $\bar{n} = (0, 1, \mathbf{0}_T)$ is the unit vector in the “-” direction, $\xi = 2x - 1$ and $\mu_M = m_M^2 / (m_{q_{f_1}} + m_{q_{f_2}})$, one obtains the final formula for a hard meson form factor up to twist-3 corrections given by [63,65]

$$\begin{aligned} F_M^{\text{hard}}(Q^2) &= F_M^{(t=2)}(Q^2) + F_M^{(t=3)}(Q^2) \\ &= 32\pi Q^2 C_F \int_0^1 dx dy \int_0^\infty b_1 db_1 b_2 db_2 \alpha_s(t) \left[\frac{x}{2} \tilde{\mathcal{P}}_{2,M}(x, b_1, 1/b_1, \mathcal{M}_q) \tilde{\mathcal{P}}_{2,M}(y, b_2, 1/b_2, \mathcal{M}_q) \right. \\ &\quad + \frac{\mu_M^2}{Q^2} (\bar{x} \tilde{\mathcal{P}}_{3,M}^p(x, b_1, 1/b_1, \mathcal{M}_q) \tilde{\mathcal{P}}_{3,M}^p(y, b_2, 1/b_2, \mathcal{M}_q) + \frac{(1+x)}{6} \tilde{\mathcal{P}}_{3,M}^p(x, b_1, 1/b_1, \mathcal{M}_q) \tilde{\mathcal{P}}_{3,M}^{\sigma'}(y, b_2, 1/b_2, \mathcal{M}_q) \\ &\quad \left. + \frac{1}{2} \tilde{\mathcal{P}}_{3,M}^p(x, b_1, 1/b_1, \mathcal{M}_q) \tilde{\mathcal{P}}_{3,M}^\sigma(y, b_2, 1/b_2, \mathcal{M}_q) \right] H(x, y, Q, b_1, b_2) \prod_{i=1}^2 S_i(x_i) S_i(\bar{x}_i) \exp[-S(x, y, b_1, b_2, Q)]; \\ \bar{x}_i &= 1 - x_i. \end{aligned} \quad (46)$$

Here, we have assumed a similar Gaussian ansatz in the transverse momentum distribution of the modified twist-3 wave functions:

$$\begin{aligned} \tilde{\mathcal{P}}_{3,M}^p(x_i, b_i, 1/b_i, \mathcal{M}_q) &= A_{3,M}^p \phi_{3,M}^p(x_i, 1/b_i) \\ &\quad \times \exp \left[-\frac{(\beta_{3,M}^p)^2 \mathcal{M}_q^2}{x_i(1-x_i)} \right] \\ &\quad \times \exp \left[-\frac{b_i^2 x_i(1-x_i)}{4(\beta_{3,M}^p)^2} \right], \\ \tilde{\mathcal{P}}_{3,M}^\sigma(x_i, b_i, 1/b_i, \mathcal{M}_q) &= A_{3,M}^\sigma \phi_{3,M}^\sigma(x_i, 1/b_i) \\ &\quad \times \exp \left[-\frac{(\beta_{3,M}^\sigma)^2 \mathcal{M}_q^2}{x_i(1-x_i)} \right] \\ &\quad \times \exp \left[-\frac{b_i^2 x_i(1-x_i)}{4(\beta_{3,M}^\sigma)^2} \right]. \end{aligned}$$

The hard kernel H and the Sudakov exponent S are given by Eqs. (41) and (42), respectively. The above formula is used to evaluate the pion and kaon hard form factors using the twist-2 DAs, Eqs. (8) and (15), respectively, and twist-3 DAs provided in Appendix A. The $S_i(x_i)$ are *jet functions*, defined as eikonalized matrix elements of quark fields attached by a Wilson line, arising from another kinematic resummation scheme called the *threshold resummation*, as introduced in Refs. [95,96]. The modified treatment of the collinear factorization prescription works reasonably well

for the twist-2 case, but for the twist-3 case, the Sudakov suppression factor may still not be effective enough in shielding the nonperturbative enhancements due to endpoint singularities. These are kinematic singularities of the scattering amplitude when the longitudinal momentum fraction x of the valence partons (quarks) goes to 0, 1. Therefore, in addition there is a need to sum up the collinear double logarithms of the type $\alpha_s \ln^2 x$ to all orders, which are then collected into these jet functions. The exact form of $S_i(x_i)$ involves a one-parameter integration, but for the sake of numerical calculations, it is convenient to take the simple parametrization, as proposed in Refs. [95,96]:

$$S_i(x_i) = \frac{2^{1+2c} \Gamma(3/2 + c)}{\sqrt{\pi} \Gamma(1 + c)} [x_i(1 - x_i)]^c, \quad (48)$$

where the parameter $c \approx 0.3$ for light pseudoscalar mesons like the pion and kaon. The jet functions vanish at the endpoints and modify the endpoint behavior of the DAs, providing enough suppression to damp the artificial effect of endpoint singularities.

B. Soft contributions via local duality

The perturbative predictions for the pion form factor are known to be relatively small for phenomenological low momentum transfers ($Q^2 \leq 10 \text{ GeV}^2$) [49–51,70,79,84,86], as is also evident from our analysis in the next section. Clearly, there is the need for including

nonfactorizable soft contributions to explain the experimental data. The factorization ansatz, Eq. (2), holds for large momentum transfers under the assumption that only the contributions from valence parton states dominate. This approximation no longer holds true at small momenta when contributions from higher Fock states with more than valence partons become significant. In addition, there could be nonperturbative enhancements from the so-called *Feynman mechanism*, which corresponds to selecting a hadronic configuration in which one of the valence partons carries almost the entire hadron momenta. Unfortunately, due to the complexity of soft QCD processes, there are no unambiguous ways to calculate these contributions analytically using the parton picture and Feynman diagrammatics, other than using theoretical models for the DAs. In this paper, we follow the local duality (LD) approach from QCD sum rules as in Ref. [62], where the same problem is addressed without a direct reference to DAs. In this section, we simply use the result for the soft form factor derived in the LD approach:

$$F_M^{\text{soft}}(Q^2) = F_M^{\text{LD}}(Q^2) = 1 - \frac{1 + 6s_0(Q^2)/Q^2}{(1 + 4s_0(Q^2)/Q^2)^{3/2}}. \quad (49)$$

The *duality interval* s_0 encodes the nonperturbative information about higher excited states and continuum contributions and is given by

$$s_0(Q^2) = 4\pi^2 f_M^2 \left(1 + \frac{\alpha_s(Q^2)}{\pi}\right). \quad (50)$$

Expanding in inverse powers of Q gives $F_M^{\text{soft}}(Q^2) \sim 1/Q^4$ for large Q^2 and is thus expected to be subleading compared to the leading perturbative contribution from Eq. (26). Nevertheless, at low and moderate momentum transfers the soft contributions turn out to be very significant in obtaining a good agreement with the experimental data. This fact is clearly revealed in our analysis in the next section.

Next we add together the hard and the soft contributions to obtain the total contributions to the electromagnetic form factor $F_M(Q^2)$. Here, it is necessary to ensure that the respective contributions lie within their domains of validity to minimize the possibility of double counting. This technique, as introduced in Ref. [62], employs gauge invariance that protects the value $F_M(0) = 1$, through the vector Ward identity relating a 3-point Green function to a 2-point Green function at zero momentum transfer, i.e., $F_M^{\text{LD}}(Q^2 = 0) = 1$. This implies that $F_M^{\text{hard}}(Q^2 = 0) = 0$. A “smooth” transition from the hard to the soft behavior is then ensured by a *matching ansatz* from the large Q^2 behavior [arising from $F_M^{\text{hard}}(Q^2)$] to the low Q^2 behavior [arising from $F_M^{\text{soft}}(Q^2)$]. This can be done by introducing a mass scale M_0 which in the LD approach should be identified with the threshold $M_0^2 = 2s_0$. The twist-2 part of the hard form factor $F_M^{(t=2)}(Q^2)$ is then modified following Ref. [62],

$$F_M^{(t=2)}(Q^2) \rightarrow \left(\frac{Q^2}{2s_0(Q^2) + Q^2}\right)^2 F_M^{(t=2)}(Q^2). \quad (51)$$

However, for the twist-3 case, the “matching function” $\Phi(z) = 1/(1+z)^2$, with $z = Q^2/M_0^2$, is insufficient to ensure the Ward identity at $Q^2 = 0$. To correct for the singular ($\sim 1/Q^4$) behavior, we make a similar modification of the twist-3 part via the replacement

$$F_M^{(t=3)}(Q^2) = \tilde{F}_M^{(t=3)}(Q^2) \frac{M_0^4}{Q^4} \rightarrow \tilde{F}_M^{(t=3)}(Q^2) \frac{M_0^4}{M_0^4 + Q^4} \quad (52)$$

with the choice of the matching function $\tilde{\Phi}(z) = 1/(1+z^2)^2$. This yields the Ward identity corrected twist-3 part:

$$F_M^{(t=3)}(Q^2) \rightarrow \left(\frac{Q^4}{4s_0^2(Q^2) + Q^4}\right)^2 F_M^{(t=3)}(Q^2). \quad (53)$$

Finally, we arrive at our expression for the total electromagnetic form factor for a charged meson $M(\pi^\pm, K^\pm)$, valid for all values of Q^2 ; it is given by

$$F_M(Q^2) = 1 - \frac{1 + 6s_0(Q^2)/Q^2}{(1 + 4s_0(Q^2)/Q^2)^{3/2}} + \left(\frac{Q^2}{2s_0(Q^2) + Q^2}\right)^2 F_M^{(t=2)}(Q^2) + \left(\frac{Q^4}{4s_0^2(Q^2) + Q^4}\right)^2 F_M^{(t=3)}(Q^2), \quad (54)$$

where $F_M^{(t=2)}(Q^2)$ and $F_M^{(t=3)}(Q^2)$ are given by Eqs. (40) and (46), respectively.

IV. NUMERICAL RESULTS

At first, we need to determine the pion and kaon Gaussian parameters $A_{2;M}$, $A_{3;M}^p$, $A_{3;M}^\sigma$ and $\beta_{2;M}$, $\beta_{3;M}^p$, $\beta_{3;M}^\sigma$ for the twist-2 and twist-3 light-cone wave functions, respectively. For the pion, they are obtained from two constraints: first, by virtue of the leptonic decay $\pi \rightarrow \mu \nu_\mu$, we have the condition

$$\int_0^1 dx \int \frac{d^2 \mathbf{k}_T}{16\pi^3} \Psi_\pi(x, \mathbf{k}_T, \mathcal{M}_{u,d}) = \frac{f_\pi}{2\sqrt{2N_c}}, \quad (55)$$

leading to

$$A_\pi \int_0^1 dx \phi_\pi(x) \exp\left[-\frac{\beta_\pi^2 \mathcal{M}_{u,d}^2}{x(1-x)}\right] = \frac{f_\pi}{2\sqrt{6}}, \quad (56)$$

and second, from $\pi^0 \rightarrow \gamma\gamma$, we have the condition

$$\int_0^1 dx \Psi_\pi(x, \mathbf{k}_T = 0, \mathcal{M}_{u,d}) = \frac{\sqrt{2N_c}}{f_\pi}, \quad (57)$$

which implies

$$16A_\pi\beta_\pi^2\pi^2\int_0^1 dx\frac{\phi_\pi(x)}{x(1-x)}\exp\left[-\frac{\beta_\pi^2\mathcal{M}_{u,d}^2}{x(1-x)}\right]=\frac{\sqrt{6}}{f_\pi}, \quad (58)$$

where we use the constituent quark mass $\mathcal{M}_{u,d} = 0.33$ GeV for both the u and d valence quarks in the pion. In the case of the kaon, first from the leptonic decay $K \rightarrow \mu\nu_\mu$, we have the constraint

$$A_K\int_0^1 dx\phi_K(x)\exp\left[-\beta_K^2\left(\frac{\mathcal{M}_s^2}{x}+\frac{\mathcal{M}_{u,d}^2}{1-x}\right)\right]=\frac{f_K}{2\sqrt{6}}. \quad (59)$$

As for the second constraint, no straightforward condition like Eq. (57) could be obtained for the kaon. On the other hand, by virtue of SU(3) isospin symmetry, it is reasonable to make an assumption that for the kaon the average transverse momentum squared of the valence partons defined by

$$\langle\mathbf{k}_T^2\rangle_K=\frac{\int dx\int d^2\mathbf{k}_T|\mathbf{k}_T^2|\Psi_K(x,\mathbf{k}_T,\mathcal{M}_{u,d,s})^2}{\int dx\int d^2\mathbf{k}_T|\Psi_K(x,\mathbf{k}_T,\mathcal{M}_{u,d,s})^2} \quad (60)$$

has about the same value as in the case of the pion. We have checked that for both the twist-2 and twist-3 pion wave functions $\langle\mathbf{k}_T^2\rangle_\pi^{1/2} \approx 0.35$ GeV. This yields our second condition for determining the wave function parameters:

$$(0.35)^2 \approx \frac{1}{2\beta_K^2}\frac{\int_0^1 dx\phi_K^2(x)\exp[-2\beta_K^2(\frac{\mathcal{M}_s^2}{x}+\frac{\mathcal{M}_{u,d}^2}{1-x})]}{\int_0^1 dx\frac{\phi_K^2(x)}{x(1-x)}\exp[-2\beta_K^2(\frac{\mathcal{M}_s^2}{x}+\frac{\mathcal{M}_{u,d}^2}{1-x})]}, \quad (61)$$

where $\mathcal{M}_s = 0.45$ GeV is used as the constituent s -quark mass and the full light-cone kaon wave function is given by

$$\Psi_K(x,\mathbf{k}_T,\mathcal{M}_{u,d,s})=\frac{16\pi^2\beta_K^2A_K}{x(1-x)}\phi_K(x)\times\exp\left[-\beta_K^2\left(\frac{\mathbf{k}_T^2+\mathcal{M}_s^2}{x}+\frac{\mathbf{k}_T^2+\mathcal{M}_{u,d}^2}{1-x}\right)\right] \quad (62)$$

with x being the longitudinal momentum fraction of the s quark. For our numerical analysis we use typical ‘‘double-humped’’ type [71–73] DAs $\phi_{\pi,K}(x,\mu^2)$, derived in the framework of QCD sum rules [35,36,38]. Note that we have considered $N_c = 3$ in the expressions for the DAs. In Figs. 1 and 2, we display the twist-2 and twist-3 light-cone wave functions for the pion and kaon, respectively, along with their corresponding asymptotic wave functions. Note that the plots exclude the normalization factors of $\frac{1}{2\sqrt{6}}$ and $\frac{1}{4\sqrt{6}}$ for the individual DAs to facilitate comparison with one another. All the DAs are defined at the scale $\mu_0 = 1$ GeV. The twist-2 and twist-3 DA input parameters are taken from Table 3 of Ref. [38], which we again provide in

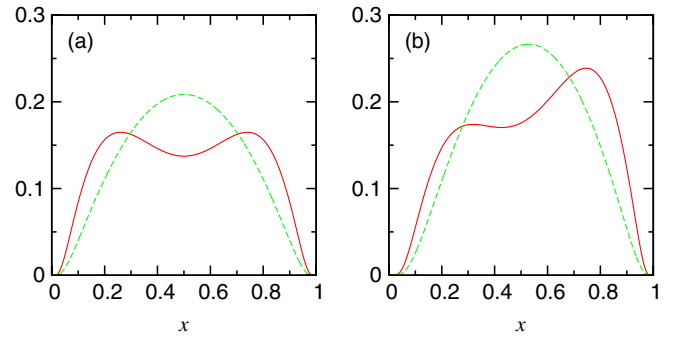


FIG. 1 (color online). Twist-2 light-cone wave functions for (a) the pion $\tilde{\mathcal{P}}_{2;\pi}$ and (b) the kaon $\tilde{\mathcal{P}}_{2;K}$ (solid lines), along with the wave functions corresponding to the respective asymptotic DAs (dashed lines). The DAs are defined at the scale $\mu_0 = 1$ GeV.

Table I along with the rest of the input parameters for the wave functions. Note that for the kaon we have shown both types of wave functions, i.e., with and without including the G -parity-breaking terms.

In Refs. [35,36,38], the DAs were assumed to obey the equations of motion (EOM) of on-shell quarks for which $\mu_M = m_M^2/(m_q + m_{q,s}) \approx 1.7$ GeV was used. This is not strictly correct, since the quarks are not exactly on shell but

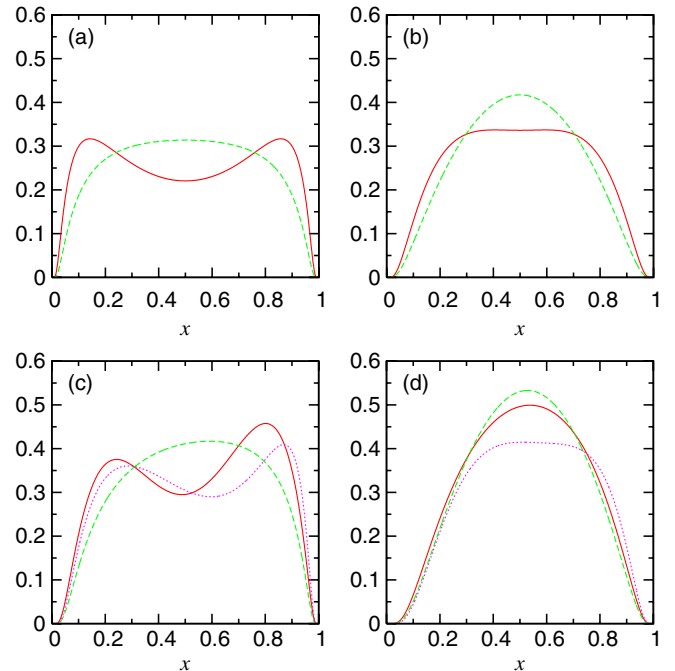


FIG. 2 (color online). Two-particle twist-3 light-cone wave functions for the pions (a) $\tilde{\mathcal{P}}_{3;\pi}^p$ and (b) $\tilde{\mathcal{P}}_{3;\pi}^\sigma$ and for the kaons (c) $\tilde{\mathcal{P}}_{3;K}^p$ and (d) $\tilde{\mathcal{P}}_{3;K}^\sigma$ with G -parity-even terms (solid lines), along with the wave functions corresponding to the respective asymptotic DAs (long dashed lines). For the kaon, the twist-3 wave functions including G -parity-odd terms are also shown (dotted lines). The DAs are defined at the scale $\mu_0 = 1$ GeV.

TABLE I. Various input hadronic parameters for twist-2 and twist-3 light-cone wave functions at $\mu_0 = 1$ GeV.

π^\pm	At $\mu_0 = 1$ GeV	K^\pm	At $\mu_0 = 1$ GeV	Units
...	...	$m_{u,d}$	5.6 ± 1.6 [38]	MeV
...	...	m_s	137 ± 27 [38]	MeV
$\mathcal{M}_{u,d}$	0.33	$\mathcal{M}_{u,d}$	0.33	GeV
...	...	\mathcal{M}_s	0.45	GeV
m_π	139	m_K	493	MeV
a_1^π	0	a_1^K	0.06 ± 0.03 [38]	...
a_2^π	0.25 ± 0.15 [38]	a_2^K	0.25 ± 0.15 [38]	...
f_π	131	f_K	$1.22 f_\pi $ [25]	MeV
$f_{3\pi}$	0.0045 ± 0.0015 [38]	f_{3K}	0.0045 ± 0.0015 [38]	GeV ²
$\omega_{3\pi}$	-1.5 ± 0.7 [38]	ω_{3K}	-1.2 ± 0.7 [38]	...
$\lambda_{3\pi}$	0	λ_{3K}	1.6 ± 0.4 [38]	...

instead confined within the hadrons. We therefore prefer using a ‘‘chiral-enhancement’’ parameter $\chi_{3M}(1 \text{ GeV}) \approx \mu_\pi \approx \mu_K$, instead of μ_M , in both the DAs and also the expression for the hard form factor, Eq. (46). Its numerical value is fixed by fitting the total form factor, Eq. (54), to the available ‘‘world data’’ for the pion [1–8]. Note that in this fitting procedure only the asymptotic forms of the twist-2 and twist-3 DAs [Eqs. (9) and (20)] were used in the pion wave functions. The running behavior $\chi_{3M}(\mu)$ is then later introduced while calculating the form factors whose RG behavior is assumed to be the same as that of μ_M (see Appendix A). In other words, this amounts to the replacement $\mu_M^2 \rightarrow \chi_{3M}(1/b_1)\chi_{3M}(1/b_2)$ in Eq. (46). In addition, as the bulk of the world pion data is concentrated in the very low-energy region where the usual running coupling rapidly diverges, we also use an analytic prescription for the QCD running coupling to prove our results. The analytic scheme was suggested originally in Ref. [91] for calculating the pion form factor and further developed in Refs. [61,62] for next-to-leading order (NLO) calculations. Here, the central idea is the removal of the explicit Landau singularity present in perturbation theory, rendering the coupling constant IR stable and reducing the IR sensitivity of perturbatively calculated hadronic observables. The scheme is also known to display higher loop stability. Now, the usual two-loop running coupling, Eq. (31), in standard pQCD can be approximately expressed via the Lambert W_{-1} function

$$\frac{\alpha_s(\mu^2)}{\pi} = -\frac{\beta_0}{\beta_1} \left[1 + W_{-1} \left(-\frac{\beta_0^2}{\beta_1 e} \left(\frac{\Lambda_{\text{QCD}}^2}{\mu^2} \right) \right) \right]^{-1}. \quad (63)$$

The extension of the above formula in analytic perturbation theory is too complicated to be evaluated exactly, and instead there is an alternate approximate expression in the $\overline{\text{MS}}$ scheme, as suggested in Ref. [90]:

$$\frac{\alpha_s^{\text{an.approx}}(\mu^2)}{\pi} = \frac{1}{\beta_0} \left[\frac{1}{l} + \frac{1}{1 - \exp(l)} \right], \quad (64)$$

$$l = \ln \left(\frac{\mu^2}{\Lambda_{\text{an}}^2} \right) + \frac{\beta_1}{\beta_0^2} \ln \sqrt{\ln^2 \left(\frac{\mu^2}{\Lambda_{\text{an}}^2} \right) + 4\pi^2}, \quad (65)$$

where Λ_{an} in the analytic scheme is the analog of Λ_{QCD} in the usual perturbation theory and is chosen to be around 0.4 GeV for $N_f = 3$. We use this formula for the analytic coupling in our calculations. The simple one-parameter fitting of the total form factor to the experimental data gives the best fit values of 1.2 GeV and 1.4 GeV for the usual and analytic QCD coupling schemes, respectively. Here, we choose the average value $\chi_{3M} = 1.3$ GeV for both the schemes, and generously consider the resulting difference from the phenomenological value of 1.7 GeV to contribute to the theoretical error, i.e., ± 0.4 GeV. Note that the fitting takes into account the individual error bars of the data points.

Finally, following Ref. [96] the Sudakov suppression factor $\exp(-s(XQ, 1/b))$ is set to unity for a small transverse separation ‘‘ b ’’ between the valence quarks, i.e., whenever $b < \sqrt{2}/(XQ)$. Also, to avoid probing into certain kinematic regions where $\exp(-S)$ may become greater than unity, causing an enhancement instead of a suppression, $\exp(-S)$ is set to 1 for $S < 0$.

A. The pion form factor

Using the DAs in Appendix A, we evaluated the total electromagnetic form factor for the pion, Eq. (54), using both the usual two-loop QCD running coupling, Eq. (31), and the analytical prescription, Eq. (64). Figure 3 shows our results for the total form factor, along with the experimental ‘‘world data’’ [1–8] for the pion. The plots correspond to $\Lambda_{\text{QCD}} = 0.2$ GeV and $\Lambda_{\text{an}} = 0.4$ GeV, respectively. It appears that the full twist-3 calculations improve the agreement with experimental data to a much better extent at intermediate energies down to around 1–2 GeV² than for the twist-2 case. Note that in the usual perturbative scheme, as $Q^2 \rightarrow 0$ the total form factor becomes very unpredictable and starts oscillating between

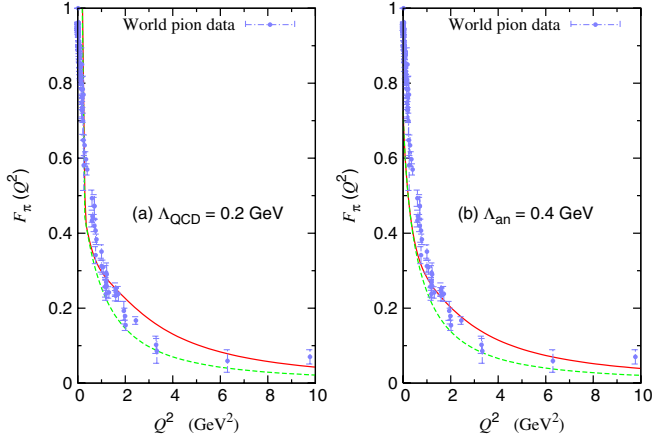


FIG. 3 (color online). The total electromagnetic pion form factor at the twist-2 level (soft + twist-2), denoted by the dashed lines, and at the twist-3 level (soft + twist-2 + twist-3), denoted by the solid lines, with (a) the usual QCD running coupling and (b) the analytical QCD running coupling. The world pion data are taken from Refs. [1–8].

large values although $F_\pi(Q^2 = 0) = 1$, satisfying the Ward identity. This clearly signals the breakdown of perturbation theory at such small momentum transfers.

To study the contributions of endpoint effects and to distinguish individual soft and hard contributions, it is more useful to study the variation of the scaled pion form factor $Q^2 F_\pi$ with Q^2 . In Fig. 4, we show the individual contributions of the twist-2 and twist-3 power corrections to the scaled hard pion form factor over a wide range of momentum transfers for the usual QCD coupling. Clearly, the twist-3 contributions are seen to be significantly larger than the leading twist-2 counterparts at low momentum transfers, supporting the claims made in [26,28,29,58,63,65]. In fact, it is interesting to see the endpoint enhancement in the twist-3 amplitudes much more explicitly if one rather considered only the collinear DAs to calculate the form factors in the usual perturbation theory, without considering the full transverse momentum dependence (e.g., the BHL ansatz) in the meson wave functions, as originally done in Ref. [96]. In other words, one simply makes the replacement $\tilde{\mathcal{P}}_M(x) \rightarrow \phi_M(x)$ in calculating the hard form factor. The inclusion of the transverse momenta and constituent quark masses in the wave function provides a natural cutoff for the soft and endpoint enhancements. Similar behavior can also be observed in the analytic case where the enhancement being less expressed has not been displayed in this work. These facts suggest that the modified collinear factorization scheme, including explicit transverse degrees of freedom with Sudakov suppression, which works well for the twist-2 case is not very effective at the twist-3 level in shielding such artificial nonperturbative enhancements at low momenta. To improve this situation, especially for the results obtained in the usual perturbative scheme, we use threshold resummation which, along with Sudakov suppression,

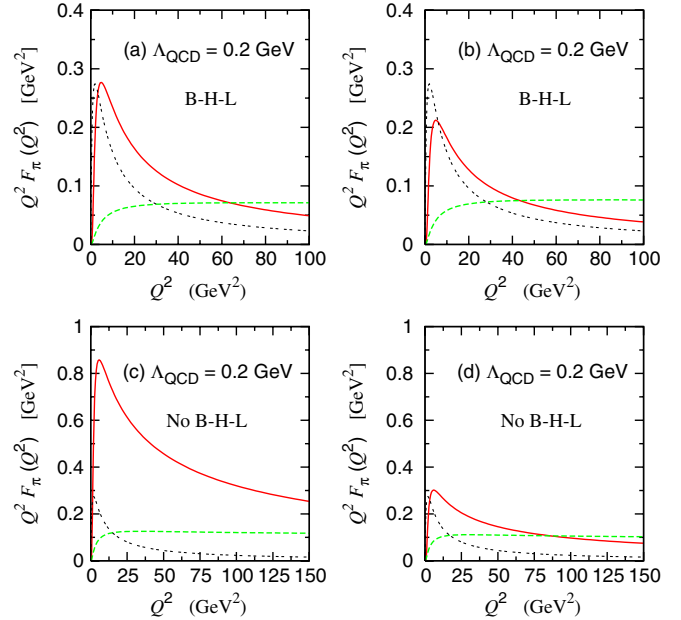


FIG. 4 (color online). Twist-2 (long dashed lines) and twist-3 (solid lines) corrections to the scaled hard pion form factor with the usual QCD running coupling. Plots (a) and (b) are obtained using BHL ansatz, while (c) and (d) are obtained with $\tilde{\mathcal{P}}_M(x) \rightarrow \phi_M(x)$. Also, plots (a) and (c) do not include threshold resummation in the hard contributions, which are included in (b) and (d). The soft corrections (short dashed lines) are also shown.

provides large damping of the endpoint effects in the twist-3 amplitude. The twist-2 part, on the other hand, remains mostly unaltered, if not slightly enhanced due to the threshold resummation, especially in the low-energy region. Note that in this respect the use of threshold resummation in the analytic scheme is somewhat redundant and has little effect on both the twist corrections. Finally, as expected, one observes that the twist-3 corrections fall off rapidly with increasing Q^2 and, beyond a certain point, fall below the twist-2 corrections. At asymptotically large momentum transfers, only the twist-2 contributions are expected to dominate.

Our final results for the scaled pion form factor are summarized in Figs. 5 and 6. We use both the usual and the analytic QCD running couplings and compare our results with the available experimental pion data with increasing error bars towards intermediate energies. The individual soft and hard contributions along with the total contribution are shown. Clearly, contrary to the earlier claims made in Ref. [59], the twist-2 hard form factor is far too small in the phenomenologically accessible region to explain the data. One must therefore look for other possibilities like nonperturbative higher-twist effects and soft contributions. Interestingly, it is seen that the soft dynamics largely dominate the low-energy region below 10–16 GeV^2 but rapidly fall off in the asymptotic region. The contributions from the twist-3 corrections turn out to be significantly large in the moderate range of energies

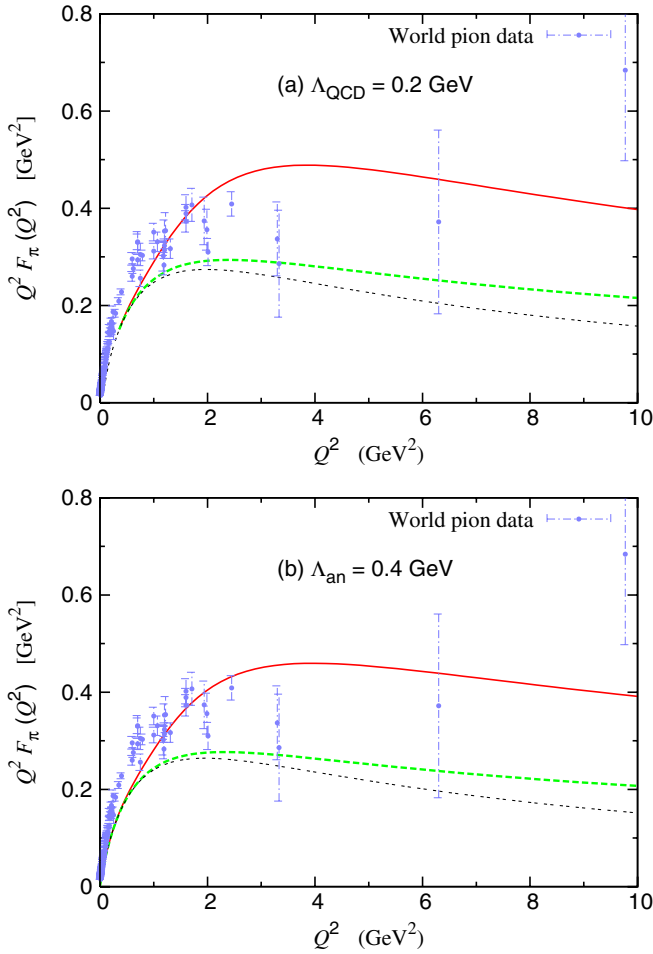


FIG. 5 (color online). Scaled total electromagnetic form factor for the pion with (a) the usual QCD running coupling and (b) the analytical running coupling in the low and intermediate-energy regime. The solid line represents the full twist-3 result (soft + twist-2 + twist-3), the long dashed lines represent the twist-2 result (soft + twist-2), and the soft corrections are indicated by the short dashed lines. The world pion data are taken from Refs. [1–8].

below 100 GeV^2 , but eventually the hard twist-2 contributions solely determine the asymptotic trend beyond $Q^2 \approx 100\text{--}150 \text{ GeV}^2$.

As evident from the figures, the total scaled pion form factor (solid lines) up to twist-3 corrections displays an obvious improvement of the overall agreement with experimental data compared to the twist-2 scaled form factor (dashed lines). To some extent, it is somewhat surprising to see that, in combination with the soft contributions, the modified resummed pQCD with the usual QCD coupling could work so well as low as $Q^2 \approx 0.25 \text{ GeV}^2$, far lower than previously envisaged. To this end, we display the results in the analytic scheme to confirm our results. The analytical prescription is known to reduce the scheme and renormalization scale dependence, largely increasing the stability of solutions [62]. Accordingly, there is some confidence in our displayed results. The results obtained in

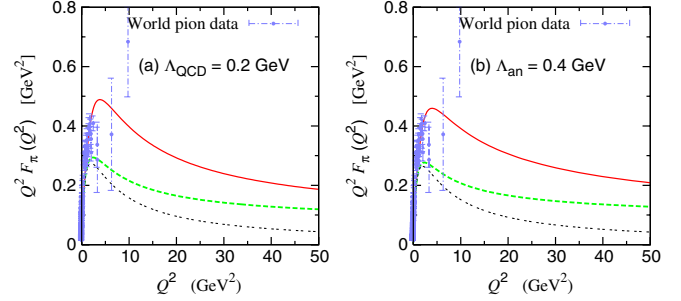


FIG. 6 (color online). Scaled total electromagnetic form factor for the pion with (a) the usual QCD running coupling and (b) the analytical running coupling over a wider range of intermediate energies. The solid line represents the full twist-3 result (soft + twist-2 + twist-3), the long dashed lines represent the full twist-2 result (soft + twist-2), and the soft corrections are indicated by the short dashed lines. The world pion data are taken from Refs. [1–8].

both schemes not only show a striking similarity even at sufficiently low momentum transfers, but they also show a good agreement with the available pion form-factor data. However, whether or not such an agreement is merely accidental is a matter of debate. There may still be substantial subleading contributions, e.g., from a full NLO calculation in the strong QCD coupling constant including subleading twists and intrinsic transverse momenta for the hard scattering kernel and the DAs, or from higher order Fock states and helicity components in the light-cone DAs. Note that a NLO calculation in the strong QCD coupling constant was done in Ref. [61] where the corrections to the twist-2 pion form factor were found to be quite large. A full NLO calculation for subleading twists, including also the transverse momentum dependence, is, however, still missing. In Ref. [64], contributions of higher helicity states were found to lower the total pion form factor significantly. Hence, without systematically taking all of these effects into account, which is beyond the scope of the paper, no definitive statement can be made as to how well our results agree with the data. Moreover, the available data themselves have very low statistics at intermediate energy and are plagued by large uncertainties. It is therefore difficult to give a proper theoretical error estimate of our results, when the asymptotic formalism is itself largely unreliable in the region of our interest. What we have done in this paper is a combination of model and pQCD calculations. It may thus be worth using the estimates for the ranges over which the input parameters of the DAs, namely, $\mu_\pi(\chi_{3\pi})$, $f_{3\pi}$, $\omega_{3\pi}$, and a_2^π , vary (given in Tables I and II), in computing our theoretical error. In addition, we allow a variation of $\pm 0.05 \text{ GeV}$ for both Λ_{QCD} and Λ_{an} . We used a Monte Carlo technique to generate a Gaussian “ 1σ ” spread of the scaled form factor for various Q^2 values about a central mean. The error estimate displayed in Fig. 7 shows our maximum theoretical error to be about 10% for the usual QCD coupling and somewhat less for the analytic coupling.

TABLE II. Various determined hadronic parameters for twist-2 and twist-3 light-cone wave functions at $\mu_0 = 1$ GeV. The numbers in the parentheses correspond to values for the asymptotic wave functions.

π^\pm	G (even)	K^\pm	G (even)	G (even + odd)	Units
$A_{2,\pi}$	1.69(1.66) _{as}	$A_{2,K}$	2.06(2.07) _{as}	2.06(2.07) _{as}	...
$A_{3,\pi}^p$	3.76(3.59) _{as}	$A_{3,K}^p$	4.40(4.56) _{as}	4.35(4.56) _{as}	...
$A_{3,\pi}^\sigma$	3.37(3.33) _{as}	$A_{3,K}^\sigma$	4.16(4.14) _{as}	4.06(4.14) _{as}	...
$(\beta_{2,\pi}^p)^2$	0.76(0.87) _{as}	$(\beta_{2,K}^p)^2$	0.78(0.89) _{as}	0.78(0.89) _{as}	GeV ⁻²
$(\beta_{3,\pi}^p)^2$	0.62(0.74) _{as}	$(\beta_{3,K}^p)^2$	0.70(0.79) _{as}	0.65(0.79) _{as}	GeV ⁻²
$(\beta_{3,\pi}^\sigma)^2$	0.81(0.87) _{as}	$(\beta_{3,K}^\sigma)^2$	0.88(0.89) _{as}	0.84(0.89) _{as}	GeV ⁻²
$\chi_{3\pi}^{\text{fit}}$	1.3 ± 0.4	χ_{3K}^{fit}	1.3 ± 0.4	1.3 ± 0.4	GeV

B. The kaon form factor

We conclude the section on the numerical analysis by displaying our predictions for the kaon form factor, applying the same techniques as for the case of the pion form factor. The twist-2 and twist-3 light-cone wave functions for the kaon have the general form in the transverse b space given by

$$\begin{aligned} \tilde{\mathcal{P}}_K(x, b, 1/b, \mathcal{M}_{u,d,s}) &= A_K \phi_K(x, 1/b) \\ &\times \exp\left[-\frac{b^2 x(1-x)}{4\beta_K^2}\right] \\ &\times \exp\left[-\beta_K^2\left(\frac{\mathcal{M}_s^2}{x} + \frac{\mathcal{M}_{u,d}^2}{1-x}\right)\right], \end{aligned} \quad (66)$$

where we used the twist-3 chiral-enhancement parameter $\chi_{3K} = 1.3$ GeV and the experimental estimate for the kaon

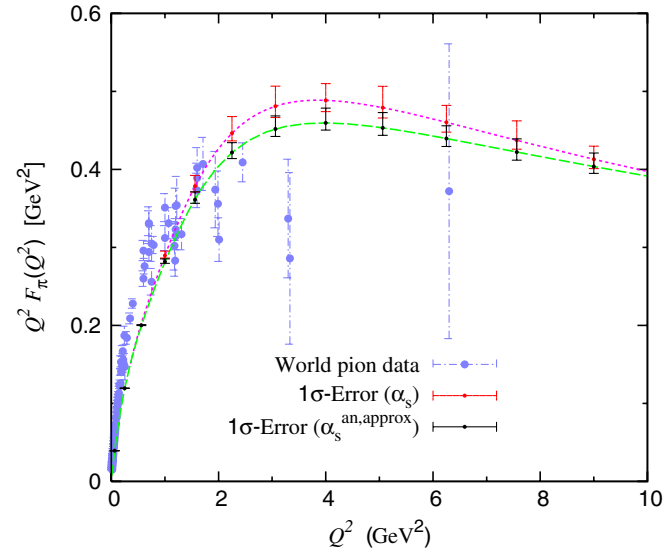


FIG. 7 (color online). Theoretical 1σ error for the scaled total pion form factor due to the variation of the input parameters for the DAs ($\chi_{3\pi}$, $f_{3\pi}$, $\omega_{3\pi}$, and a_2^T) and $\Lambda_{\text{QCD,an}}$. The lines correspond to the mean values of the parameters using the usual (dotted line) and the analytic (broken line) QCD coupling schemes, respectively. The error bars for the experimental data points [1–8] are also shown.

decay constant $f_K \approx 1.22f_\pi$ [25]. Here, we also take $\Lambda_{\text{QCD}} = 0.2$ GeV and $\Lambda_{\text{an}} = 0.4$ GeV for the respective running couplings in the $\overline{\text{MS}}$ scheme. The results are

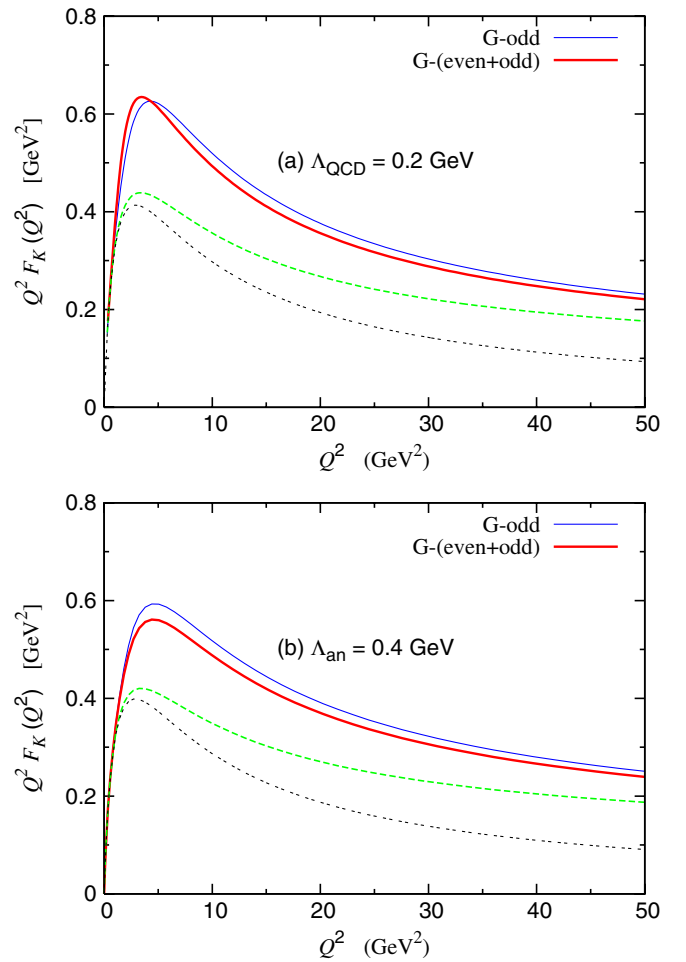


FIG. 8 (color online). Scaled total electromagnetic form factor for the kaon with the usual QCD running coupling (upper plot) and the analytical running coupling (lower plot) for intermediate energies. The solid lines represent the full twist-3 result (soft + twist-2 + twist-3), the long dashed lines represent the twist-2 result (soft + twist-2), and the soft corrections are indicated by the short dashed lines. For the full twist-3 case, both the results, i.e., with and without the G -parity-breaking terms in the DAs, are shown.

summarized in Fig. 8 for intermediate energies. The solid line represents the total scaled form factor in each case. Here, our results for the kaon form factor must be considered preliminary. Because of the complete absence of experimental data at intermediate energies, we are unable to make any meaningful phenomenological comparison. The presently available kaon data have very poor statistics and have hardly been measured above 0.2 GeV^2 . Hence, we do not show the experimental data points in the form-factor plots. With the availability of better quality data in the future, there could be plenty of room for further improvements, for instance, the extension of the above results to include a full NLO calculation for subleading twists or higher helicity and Fock state contributions.

V. DISCUSSION AND CONCLUSION

For the past two decades the electromagnetic meson form factors have been the subject of intensive theoretical and experimental scrutiny, and yet there is still not a universally accepted framework for their description. Presently, reliable experimental data are available only for the pions which are entirely concentrated at very low energies with very poor statistics at intermediate energies. The low-energy part of the data is best explained by the standard VMD model, showing no apparent trace of pQCD behavior, which is expected only at very high energies. Very many attempts have been made to predict the onset of the perturbative behavior for the pion form factor. The modified or resummed valence pQCD with factorization appears to show some attractive features to enable pQCD calculations to be valid in a self-consistent way even at very moderate energies. Whether this is true will only be confirmed when data with better statistics at higher momentum transfers become available in the future. At the same time, the onset of the perturbative behavior being very slow, it is still unclear whether the leading order perturbative calculations could be expected to be precise even at the highest accessible energies. In this paper, with the help of (a) the double-humped-type DAs and (b) the modified transverse (k_T) factorization scheme, incorporating both Sudakov suppression and threshold resummation, we got rid of nonperturbative endpoint enhancements. This enlarges the scope of applicability of resummed pQCD, independent of the coupling scheme, to a much wider range of intermediate energies, if not down to a few GeVs, as demonstrated in this paper. By a simple adjustment of only the chiral-enhancement parameter $\chi_{3\pi}$, a good agreement with the experimental data was obtained.

As for the scaled pion form factor, we found that the leading order pQCD contributions potentially undermine the agreement with the available low-energy data and are only trustworthy in the hard-energy regime: even from a very conservative point of view, Q^2 should be bigger than 4 GeV^2 . At low momentum transfers, the nonperturbative

contributions dominate, being larger than the hard (twist-2) contributions at least by a factor of 2. In fact, below 4 GeV^2 , 60%–70% of the available data are already accounted for by the soft contributions. In addition, we also needed the twist-3 power corrections to explain the remaining discrepancy. However, at larger energies (say, $Q^2 > 50\text{--}100 \text{ GeV}^2$), both the soft and the twist-3 contributions rapidly fall off, and eventually the twist-2 form factor dominates asymptotically. Similar conclusions, albeit being preliminary, are drawn for the kaon form factor, although it seems that the onset of the perturbative behavior occurs at slightly larger momentum transfers than for the case of the pion. Of course, as we mentioned earlier, we still need to investigate the nature of the contributions that may arise from a full systematic NLO calculation with subleading twists and intrinsic transverse momenta, or from the inclusion of higher helicity and Fock states. With the availability of better quality data in the future, such analyses may be necessary to make definite conclusions.

In summary, although the quality of present experimental form-factor data does not allow a definitive conclusion, one can expect that the nonperturbative soft contributions and higher-twist power corrections to the form factors play an important role at phenomenologically accessible momentum transfers. Thus, more work needs to be done on both the theoretical and experimental sides to obtain more conclusive results and push the frontiers of our knowledge on confinement dynamics to the study of higher order and nonperturbative contributions to exclusive processes.

ACKNOWLEDGMENTS

The authors would like to thank Alexander Bakulev, Pankaj Jain, Alexander Lenz, Seregy Mikhailov, Sabyasachi Mishra, Ingo Sick, Ritesh Singh, Nikolaos Stefanis, and Xing-Gang Wu for interesting discussions and comments. One of the authors (U.R.) would like to convey special thanks to Professor Dirk Trautmann and Professor Friedel Thielemann for their hospitality and financial support at the University of Basel. This work was supported by the Swiss National Science Foundation (SNSF) under Contract No. 200020-111705.

APPENDIX A: TWO-PARTICLE TWIST-3 DISTRIBUTION AMPLITUDES

The twist-3 DAs are obtained by an expansion over conformal spins. At next-to-leading order, the 2-particle DAs $\phi_{3,M}^p$ and $\phi_{3,M}^\sigma$ [including meson-mass corrections that break chiral symmetry at $\mathcal{O}(m_s + m_q)$ in the SU(3) case while preserving G -parity] are given in terms of the Gegenbauer polynomials $C_n^{1/2}$ and $C_n^{3/2}$, respectively [35,36], as

$$\begin{aligned}\phi_{3;M}^p(x, \mu^2) &= \frac{f_M}{4\sqrt{2N_c}} \left\{ 1 + \left(30\eta_{3M}(\mu^2) - \frac{5}{2}\rho_M^2(\mu^2) \right) C_2^{1/2}(\xi) \right. \\ &\quad \left. + \left(-3\eta_{3M}(\mu^2)\omega_{3M}(\mu^2) - \frac{27}{20}\rho_M^2(\mu^2) - \frac{81}{10}\rho_M^2(\mu^2)a_2^M(\mu^2) \right) C_4^{1/2}(\xi) \right\}, \\ \phi_{3;M}^\sigma(x, \mu^2) &= \frac{3f_M}{2\sqrt{2N_c}} x(1-x) \left\{ 1 + \left(5\eta_{3M}(\mu^2) - \frac{1}{2}\eta_{3M}(\mu^2)\omega_{3M}(\mu^2) - \frac{7}{20}\rho_M^2(\mu^2) - \frac{3}{5}\rho_M^2(\mu^2)a_2^M(\mu^2) \right) C_2^{3/2}(\xi) \right\}\end{aligned}\quad (\text{A1})$$

with

$$\eta_{3M} = \frac{f_{3M}}{f_M} \frac{1}{\mu_M}, \quad \rho_M = \frac{m_M}{\mu_M}; \quad M = \pi^\pm, K^\pm \quad (\text{A2})$$

where the nonperturbative parameters f_{3M} and ω_{3M} , respectively, are defined by the following matrix elements of local twist-3 operators:

$$\begin{aligned}\langle 0 | \bar{q}_{f_1} \sigma_{\mu\nu} \gamma_5 g_s G_{\alpha\beta} q_{f_2} | M(P) \rangle &= if_{3M} (P_\alpha P_\mu g_{\nu\beta} - P_\alpha P_\nu g_{\mu\beta} - P_\beta P_\mu g_{\nu\alpha} + P_\beta P_\nu g_{\alpha\mu}), \\ \langle 0 | \bar{q}_{f_1} \sigma_{\mu\lambda} \gamma_5 [iD_\beta, g_s G_{\alpha\lambda}] q_{f_2} - (3/7)i\partial_\beta \bar{q}_{f_1} \sigma_{\mu\lambda} \gamma_5 g_s G_{\alpha\lambda} q_{f_2} | M(P) \rangle &= \frac{3}{14} if_{3M} P_\alpha P_\beta P_\mu \omega_{3M},\end{aligned}\quad (\text{A3})$$

where $G_{\alpha\beta}$ is the gluon field tensor. The LO scale dependence of various twist-3 parameters is given by

$$\begin{aligned}\rho_M(\mu^2) &= L^{\gamma_{3;q\bar{q}}^{(0)}/\beta_0} \rho_M(\mu_0^2); \quad \gamma_{3;q\bar{q}}^{(0)} = 1, \quad \mu_M(\mu^2) = L^{\gamma_{3;\mu}^{(0)}/\beta_0} \mu_M(\mu_0^2); \\ \gamma_{3;\mu}^{(0)} = -\gamma_{3;q\bar{q}}^{(0)} &= -1, \quad \eta_{3M}(\mu^2) = L^{\gamma_{3;\eta}^{(0)}/\beta_0} \eta_{3M}(\mu_0^2); \quad \gamma_{3;\eta}^{(0)} = \frac{4}{3}C_F + \frac{1}{4}C_A, \quad \omega_{3M}(\mu^2) = L^{\gamma_{3;\omega}^{(0)}/\beta_0} \omega_{3M}(\mu_0^2); \\ \gamma_{3;\omega}^{(0)} &= -\frac{7}{24}C_F + \frac{7}{12}C_A, \quad a_2^M(\mu^2) = L^{\gamma_2^{(0)}/\beta_0} a_2^M(\mu_0^2); \quad \gamma_2^{(0)} = \frac{25}{24}C_F,\end{aligned}\quad (\text{A4})$$

where $L = \alpha_s(\mu^2)/\alpha_s(\mu_0^2)$, $C_F = (N_c^2 - 1)/2N_c$, $C_A = N_c$, and $\mu_0 \approx 1$ GeV.

We have also considered the 2-particle twist-3 kaon DAs $\phi_{3,K}^p$ and $\phi_{3,K}^\sigma$, as given in [38], which not only include a complete set of meson-mass corrections but also G -parity-breaking terms of $\mathcal{O}(m_s - m_q)$:

$$\begin{aligned}\phi_{3;K}^p(x, \mu^2) &= \frac{f_K}{4\sqrt{2N_c}} \left\{ 1 + 3\rho_+^K(1 + 6a_2^K) - 9\rho_-^K a_1^K + \left[\frac{27}{2}\rho_+^K a_1^K - \rho_-^K \left(\frac{3}{2} + 27a_2^K \right) \right] C_1^{1/2}(\xi) \right. \\ &\quad \left. + (30\eta_{3K} + 15\rho_+^K a_2^K - 3\rho_-^K a_1^K) C_2^{1/2}(\xi) + \left(10\eta_{3K}\lambda_{3K} - \frac{9}{2}\rho_-^K a_2^K \right) C_3^{1/2}(\xi) - 3\eta_{3K}\omega_{3K} C_4^{1/2}(\xi) \right. \\ &\quad \left. + \frac{3}{2}(\rho_+^K + \rho_-^K)(1 - 3a_1^K + 6a_2^K) \ln x + \frac{3}{2}(\rho_+^K - \rho_-^K)(1 + 3a_1^K + 6a_2^K) \ln(1-x) \right\},\end{aligned}\quad (\text{A5})$$

$$\begin{aligned}\phi_{3;K}^\sigma(x, \mu^2) &= \frac{3f_K}{2\sqrt{2N_c}} x(1-x) \left\{ 1 + \frac{3}{2}\rho_+^K + 15\rho_+^K a_2^K - \frac{15}{2}\rho_-^K a_1^K + \left(3\rho_+^K a_1^K - \frac{15}{2}\rho_-^K a_2^K \right) C_1^{3/2}(\xi) \right. \\ &\quad \left. + \left(5\eta_{3K} - \frac{1}{2}\eta_{3K}\omega_{3K} + \frac{3}{2}\rho_+^K a_2^K \right) C_2^{3/2}(\xi) + \eta_{3K}\lambda_{3K} C_3^{3/2}(\xi) + \frac{3}{2}(\rho_+^K + \rho_-^K)(1 - 3a_1^K + 6a_2^K) \ln x \right. \\ &\quad \left. + \frac{3}{2}(\rho_+^K - \rho_-^K)(1 + 3a_1^K + 6a_2^K) \ln(1-x) \right\} \left(\frac{1}{1 - \rho_+} \right)\end{aligned}\quad (\text{A6})$$

with

$$\eta_{3K} = \frac{f_{3K}}{f_K} \frac{1}{\mu_K}, \quad \rho_+^K = \frac{(m_s + m_q)^2}{m_K^2}, \quad \text{and} \quad \rho_-^K = \frac{m_s^2 - m_q^2}{m_K^2}.\quad (\text{A7})$$

Note that the expression for $\phi_{3;K}^\sigma(x, \mu^2)$ is normalized to unity with an extra factor of $1/(1 - \rho_+)$, compared to that given in [38]. The nonperturbative parameters f_{3K} , ω_{3K} , and λ_{3K} are defined (e.g., K^-) by

$$\begin{aligned}
\langle 0 | \bar{u} \sigma_{\mu\nu} \gamma_5 g_s G_{\alpha\beta} s | K^-(P) \rangle &= i f_{3K} (P_\alpha P_\mu g_{\nu\beta} - P_\alpha P_\nu g_{\mu\beta} - P_\beta P_\mu g_{\nu\alpha} + P_\beta P_\nu g_{\alpha\mu}), \\
\langle 0 | \bar{u} \sigma_{\mu\lambda} \gamma_5 [i D_\beta, g_s G_{\alpha\lambda}] s - (3/7) i \partial_\beta \bar{u} \sigma_{\mu\lambda} \gamma_5 g_s G_{\alpha\lambda} s | K^-(P) \rangle &= \frac{3}{14} i f_{3K} P_\alpha P_\beta P_\mu \omega_{3K}, \\
\langle 0 | \bar{u} i \tilde{D}_\beta \sigma_{\mu\lambda} \gamma_5 g_s G_{\alpha\lambda} s - \bar{u} \sigma_{\mu\lambda} \gamma_5 g_s G_{\alpha\lambda} i \tilde{D}_\beta s | K^-(P) \rangle &= \frac{1}{7} i f_{3K} P_\alpha P_\beta P_\mu \lambda_{3K},
\end{aligned} \tag{A8}$$

where in the chiral limit the renormalization group equations at LO give

$$\begin{aligned}
\mu_K(\mu^2) &= L^{\gamma_{3;\mu}^{(0)}/\beta_0} \mu_K(\mu_0^2); & \gamma_{3;\mu}^{(0)} &= -\gamma_{3;q\bar{q}}^{(0)} = -1, & \rho_+^K(\mu^2) &= L^{\gamma_{3;\rho^+}^{(0)}/\beta_0} \rho_+^K(\mu_0^2); & \gamma_{3;\rho^+}^{(0)} &= 2\gamma_{3;q\bar{q}}^{(0)} = 2, \\
\rho_-^K(\mu^2) &= L^{\gamma_{3;\rho^-}^{(0)}/\beta_0} \rho_-^K(\mu_0^2); & \gamma_{3;\rho^-}^{(0)} &= 2\gamma_{3;q\bar{q}}^{(0)} = 2, & f_{3K}(\mu^2) &= L^{\gamma_{3;f}^{(0)}/\beta_0} f_{3K}(\mu_0^2); & \gamma_{3;f}^{(0)} &= \frac{7}{12} C_F + \frac{1}{4} C_A, \\
\omega_{3K}(\mu^2) &= L^{\gamma_{3;\omega}^{(0)}/\beta_0} \omega_{3K}(\mu_0^2); & \gamma_{3;\omega}^{(0)} &= -\frac{7}{24} C_F + \frac{7}{12} C_A, & \lambda_{3K}(\mu^2) &= L^{\gamma_{3;\lambda}^{(0)}/\beta_0} \lambda_{3K}(\mu_0^2); & \gamma_{3;\lambda}^{(0)} &= \frac{19}{48} C_F, \\
a_1^K(\mu^2) &= L^{\gamma_1^{(0)}/\beta_0} a_1^K(\mu_0^2); & \gamma_1^{(0)} &= \frac{2}{3} C_F, & a_2^K(\mu^2) &= L^{\gamma_2^{(0)}/\beta_0} a_2^K(\mu_0^2); & \gamma_2^{(0)} &= \frac{25}{24} C_F.
\end{aligned} \tag{A9}$$

But since the strange quark is massive, there is operator mixing of the ones in Eq. (A8) with that of twist-2 operators and the resulting LO renormalization group equations give the following scale dependence of the various twist-3 parameters:

$$\begin{aligned}
f_{3K}(\mu^2) &= L^{55/(36\beta_0)} f_{3K}(\mu_0^2) + \frac{2}{19} (L^{1/\beta_0} - L^{55/(36\beta_0)}) [f_K m_s](\mu_0^2) + \frac{6}{65} (L^{55/(36\beta_0)} - L^{17/(9\beta_0)}) [f_K m_s a_1^K](\mu_0^2), \\
[f_{3K} \omega_{3K}](\mu^2) &= L^{26/(9\beta_0)} [f_{3K} \omega_{3K}](\mu_0^2) + \frac{1}{170} (L^{1/\beta_0} - L^{26/(9\beta_0)}) [f_K m_s](\mu_0^2) + \frac{1}{10} (L^{17/(9\beta_0)} - L^{26/(9\beta_0)}) [f_K m_s a_1^K](\mu_0^2) \\
&\quad + \frac{2}{15} (L^{43/(18\beta_0)} - L^{26/(9\beta_0)}) [f_K m_s a_2^K](\mu_0^2), \\
[f_{3K} \lambda_{3K}](\mu^2) &= L^{37/(18\beta_0)} [f_{3K} \lambda_{3K}](\mu_0^2) - \frac{14}{67} (L^{1/\beta_0} - L^{37/(18\beta_0)}) [f_K m_s](\mu_0^2) + \frac{14}{5} (L^{17/(9\beta_0)} - L^{37/(18\beta_0)}) [f_K m_s a_1^K](\mu_0^2) \\
&\quad - \frac{4}{11} (L^{43/(18\beta_0)} - L^{37/(18\beta_0)}) [f_K m_s a_2^K](\mu_0^2).
\end{aligned} \tag{A10}$$

Finally, we present the various Gegenbauer polynomials used in the above formulas:

$$\begin{aligned}
C_1^{1/2}(\xi) &= \xi, & C_2^{1/2}(\xi) &= \frac{1}{2}(3\xi^2 - 1), & C_3^{1/2}(\xi) &= \frac{1}{2}\xi(5\xi^2 - 3), & C_4^{1/2}(\xi) &= \frac{1}{8}(35\xi^4 - 30\xi^2 + 3), \\
C_0^{3/2}(\xi) &= 1, & C_1^{3/2}(\xi) &= 3\xi, & C_2^{3/2}(\xi) &= \frac{3}{2}(5\xi^2 - 1), & C_3^{3/2}(\xi) &= \frac{5}{2}\xi(7\xi^2 - 3).
\end{aligned} \tag{A11}$$

APPENDIX B: CALCULATION OF THE SUDAKOV EXPONENT

The full expression of the Sudakov suppression factor $S(x, y, b_1, b_2, Q)$ is given by

$$\begin{aligned}
S(x, y, b_1, b_2, Q) &= s(xQ, b_1) + s(yQ, b_2) + s((1-x)Q, b_1) + s((1-y)Q, b_2) - \frac{1}{\beta_0} \ln\left(\frac{\hat{t}}{-\hat{b}_1}\right) - \frac{1}{\beta_0} \ln\left(\frac{\hat{t}}{-\hat{b}_2}\right) \\
&\quad + \frac{\beta_1}{\beta_0^3} \left[\frac{1 + \ln(-2\hat{b}_1)}{-2\hat{b}_1} - \frac{1 + \ln(2\hat{t})}{2\hat{t}} \right] + \frac{\beta_1}{\beta_0^3} \left[\frac{1 + \ln(-2\hat{b}_2)}{-2\hat{b}_2} - \frac{1 + \ln(2\hat{t})}{2\hat{t}} \right],
\end{aligned} \tag{B1}$$

where

$$\begin{aligned}
s(XQ, 1/b) = & \frac{\mathcal{A}^{(1)}}{2\beta_0} \hat{q} \ln\left(\frac{\hat{q}}{-\hat{b}}\right) + \frac{\mathcal{A}^{(2)}}{4\beta_0^2} \left(\frac{\hat{q}}{-\hat{b}} - 1\right) - \frac{\mathcal{A}^{(1)}}{2\beta_0} (\hat{b} + \hat{q}) - \left[\frac{4\mathcal{A}^{(1)}\beta_1}{16\beta_0^3} \hat{q} + \frac{2\mathcal{A}^{(1)}\beta_1}{16\beta_0^3} \ln\left(\frac{1}{2} e^{2\gamma_E - 1}\right) \right] \\
& \times \left[\frac{1 + \ln(-2\hat{b})}{-\hat{b}} - \frac{1 + \ln(2\hat{q})}{\hat{q}} \right] - \left[\frac{\mathcal{A}^{(2)}}{4\beta_0^2} - \frac{\mathcal{A}^{(1)}}{4\beta_0} \ln\left(\frac{1}{2} e^{2\gamma_E - 1}\right) \right] \ln\left(\frac{\hat{q}}{-\hat{b}}\right) - \frac{4\mathcal{A}^{(1)}\beta_1}{32\beta_0^3} \left[\ln^2(-2\hat{b}) - \ln^2(2\hat{q}) \right] \\
& + \frac{2\mathcal{A}^{(2)}\beta_1}{8\beta_0^4} \left[\frac{1 + \ln(-2\hat{b})}{-\hat{b}} - \frac{1 + \ln(2\hat{q})}{\hat{q}} \right] - \frac{2\mathcal{A}^{(2)}\beta_1}{8\beta_0^4} \hat{q} \left[\frac{1 + 2\ln(-2\hat{b})}{(-2\hat{b})^2} - \frac{1 + 2\ln(2\hat{q})}{(2\hat{q})^2} \right] \\
& - \frac{4\mathcal{A}^{(2)}\beta_1^2}{64\beta_0^6} \left[\frac{1 + 2\ln(-2\hat{b}) + 2\ln^2(-2\hat{b})}{(-2\hat{b})^2} - \frac{1 + 2\ln(2\hat{q}) + 2\ln^2(2\hat{q})}{(2\hat{q})^2} \right] \\
& + \frac{4\mathcal{A}^{(2)}\beta_1^2}{8\beta_0^6} \hat{q} \left[\frac{\frac{2}{27} + \frac{2}{9} \ln(-2\hat{b}) + \frac{1}{3} \ln^2(-2\hat{b})}{(-2\hat{b})^3} - \frac{\frac{2}{27} + \frac{2}{9} \ln(2\hat{q}) + \frac{1}{3} \ln^2(2\hat{q})}{(2\hat{q})^3} \right]. \tag{B2}
\end{aligned}$$

In the above formulas,

$$\begin{aligned}
\hat{t} = \ln\left(\frac{t}{\Lambda_{\text{QCD}}}\right); \quad t = \max(\sqrt{xy}Q, 1/b_1, 1/b_2), \quad \hat{b} = \ln(b\Lambda_{\text{QCD}}), \quad \hat{q} = \ln\left[\frac{XQ}{\sqrt{2}\Lambda_{\text{QCD}}}\right]; \\
X = x, y, (1-x) \text{ or } (1-y), \quad \mathcal{A}^{(1)} = C_F = \frac{4}{3}, \quad \mathcal{A}^{(2)} = \left(\frac{67}{27} - \frac{\pi^2}{9}\right)N_c - \frac{10}{27}N_f + \frac{8}{3}\beta_0 \ln\left(\frac{e^{\gamma_E}}{2}\right). \tag{B3}
\end{aligned}$$

-
- [1] C.N. Brown *et al.*, Phys. Rev. D **8**, 92 (1973).
[2] C.J. Babek *et al.*, Phys. Rev. D **17**, 1693 (1978).
[3] H. Ackermann *et al.*, Nucl. Phys. **B137**, 294 (1978).
[4] P. Brauel *et al.*, Z. Phys. C **3**, 101 (1979).
[5] S.R. Amendolia *et al.*, Nucl. Phys. **B277**, 168 (1986).
[6] J. Volmer, Ph.D. thesis, Vrije Universiteit, Amsterdam, 2000 (unpublished); Phys. Rev. Lett. **86**, 1713 (2001).
[7] T. Horn *et al.*, Phys. Rev. Lett. **97**, 192001 (2006).
[8] V. Tadevosyan *et al.*, Phys. Rev. C **75**, 055205 (2007).
[9] B. Zeidman *et al.*, CEBAF Experiment Report No. E91-016/1996.
[10] R. Mohring *et al.*, Phys. Rev. Lett. **81**, 1805 (1998).
[11] M. Vanderhaeghen, M. Guidal, and J.-M. Laget, Phys. Rev. C **57**, 1454 (1998).
[12] C. Bennhold and T. Mart, Phys. Rev. C **61**, 012201 (1999).
[13] R. A. Williams, Phys. Rev. C **46**, 1617 (1992).
[14] S.R. Amendolia *et al.*, Phys. Lett. B **178**, 435 (1986); Nucl. Phys. **B277**, 168 (1986).
[15] E. B. Dally *et al.*, Phys. Rev. Lett. **45**, 232 (1980).
[16] K. H. Glander *et al.*, Eur. Phys. J. A **19**, 251 (2004).
[17] J. W. C. McNabb *et al.*, Phys. Rev. C **69**, 042201(R) (2004).
[18] R. G. T. Zegers *et al.*, Phys. Rev. Lett. **91**, 092001 (2003).
[19] B.-W. Xiao and X. Qian, Eur. Phys. J. A **15**, 523 (2002).
[20] F. P. Pereira *et al.*, Phys. Part. Nucl. **36**, 217 (2005).
[21] X.-G. Wu and T. Huang, J. High Energy Phys. **04** (2008) 043.
[22] J. Bijnens and A. Khodjamirian, Eur. Phys. J. C **26**, 67 (2002).
[23] J. Botts and G. Sterman, Nucl. Phys. **B325**, 62 (1989).
[24] H.-N. Li and G. Sterman, Nucl. Phys. **B381**, 129 (1992).
[25] V.L. Chernyak and A.R. Zhitnitsky, Yad. Fiz. **31**, 1053 (1980) [JETP Lett. **25**, 510 (1977)]; Nucl. Phys. **B201**, 492 (1982); Sov. J. Nucl. Phys. **38**, 775 (1983); Nucl. Phys. **B246**, 52 (1984); Phys. Rep. **112**, 173 (1984).
[26] V.L. Chernyak, A.R. Zhitnitsky, and I.R. Zhitnitsky, Nucl. Phys. **B204**, 477 (1982).
[27] V.L. Chernyak, A.R. Zhitnitsky, and V.G. Serbo, JETP Lett. **26**, 594 (1977); Sov. J. Nucl. Phys. **31**, 552 (1980).
[28] B. V. Geshkenbeim and M. V. Terentyev, Phys. Lett. **117B**, 243 (1982); Sov. J. Nucl. Phys. **39**, 554 (1984); **39**, 873 (1984).
[29] C. S. Huang, Commun. Theor. Phys. **2**, 1265 (1983).
[30] M. Gari and N. G. Stefanis, Phys. Lett. B **175**, 462 (1986).
[31] Z. Dziembowski and L. Mankiewicz, Phys. Rev. Lett. **58**, 2175 (1987).
[32] T. Huang and Q. X. Sheng, Z. Phys. C **50**, 139 (1991).
[33] F.-G. Cao, T. Huang, and B. Q. Ma, Phys. Rev. D **53**, 6582 (1996).
[34] S. Brodsky and G.F. de Teramond, arXiv:hep-ph/0804.3562.
[35] V.M. Braun and I.E. Filyanov, Z. Phys. C **44**, 157 (1989).
[36] P. Ball, J. High Energy Phys. **01** (1999) 010.
[37] P. Ball and M. Boglione, Phys. Rev. D **68**, 094006 (2003).
[38] P. Ball, V.M. Braun, and A. Lenz, J. High Energy Phys. **05** (2006) 004.
[39] A. Khodjamirian, Th. Mannel, and M. Melcher, Phys. Rev. D **68**, 114007 (2003); **70**, 094002 (2004).
[40] C.-R. Ji and F. Amiri, Phys. Rev. D **42**, 3764 (1990).
[41] J. M. Cornwall, Phys. Rev. D **26**, 1453 (1982).
[42] C.-R. Ji, A. F. Sill, and R. M. Lombard-Nelson, Phys. Rev. D **36**, 165 (1987).
[43] W. G. Holladay, Phys. Rev. **101**, 1198 (1956).
[44] W.R. Frazer and J.R. Fulco, Phys. Rev. Lett. **2**, 365

- (1959); Phys. Rev. **117**, 1609 (1960).
- [45] J. Sakurai, *Currents and Mesons* (University of Chicago, Chicago, 1969).
- [46] B. Ananthanarayan and S. Ramanan, Eur. Phys. J. C **54**, 461 (2008).
- [47] S. J. Brodsky and G. R. Farrar, Phys. Rev. Lett. **31**, 1153 (1973); Phys. Rev. D **11**, 1309 (1975).
- [48] F. R. Farrar and D. R. Jackson, Phys. Rev. Lett. **43**, 246 (1979).
- [49] V. A. Nesterenko and A. V. Radyushkin, Phys. Lett. **115B**, 410 (1982).
- [50] V. V. Anisovich, D. I. Melikhov, and V. A. Nikonov, Phys. Rev. D **52**, 5295 (1995); **55**, 2918 (1997).
- [51] A. P. Bakulev, A. V. Radyushkin, and N. G. Stefanis, Phys. Rev. D **62**, 113001 (2000).
- [52] V. Braguta, W. Lucha, and D. Melikhov, Phys. Lett. B **661**, 354 (2008).
- [53] C. R. Ji and S. Cotanch, Phys. Rev. D **41**, 2319 (1990).
- [54] T. Gousset and B. Pire, Phys. Rev. D **51**, 15 (1995); Proceedings of the ELFE Summer School on Confinement Physics, Cambridge, 1995, pp. 111–143.
- [55] C.-R. Ji, A. Pang, and A. Szczepaniak, Phys. Rev. D **52**, 4038 (1995).
- [56] J. P. B. C. de Melo *et al.*, Phys. Rev. C **59**, 2278 (1999); Nucl. Phys. **A707**, 399 (2002).
- [57] H.-M. Choi and C.-R. Ji, Phys. Rev. D **74**, 093010 (2006); Phys. Rev. D **77**, 113004 (2008).
- [58] F.-G. Cao, Y.-B. Dai, and C.-S. Huang, Eur. Phys. J. C **11**, 501 (1999).
- [59] C. Coriano, H.-N. Li, and C. Savkli, J. High Energy Phys. **07** (1998) 008.
- [60] V. M. Braun, A. Khodjamirian, and M. Maul, Phys. Rev. D **61**, 073004 (2000).
- [61] N. G. Stefanis, W. Schroers, and H.-Ch. Kim, Eur. Phys. J. C **18**, 137 (2000).
- [62] A. P. Bakulev *et al.*, Phys. Rev. D **70**, 033014 (2004).
- [63] Z.-T. Wei and M.-Z. Yang, Phys. Rev. D **67**, 094013 (2003).
- [64] T. Huang, X.-G. Wu, and X.-H. Wu, Phys. Rev. D **70**, 053007 (2004).
- [65] T. Huang and X.-G. Wu, Phys. Rev. D **70**, 093013 (2004).
- [66] F. D. R. Bonnet *et al.* (Lattice Hadron Physics Collaboration), Phys. Rev. D **72**, 054506 (2005).
- [67] S. Hashimoto *et al.* (JLQCD Collaboration), Proc. Sci., LAT2005 (2006) 336 [arXiv:hep-lat/0510085].
- [68] D. Brömmel *et al.*, Proc. Sci., LAT2005 (2006) 360 [arXiv:hep-lat/0509133]; Eur. Phys. J. C **51**, 335 (2007).
- [69] P.-H. J. Hsu and G. T. Fleming, Proc. Sci., LAT2007 (2007) 145 [arXiv:hep-lat/0710.4538].
- [70] A. P. Bakulev and A. V. Radyushkin, Phys. Lett. B **271**, 223 (1991).
- [71] G. P. Lepage and S. J. Brodsky, Phys. Lett. **87B**, 359 (1979); Phys. Rev. Lett. **43**, 545 (1979); Phys. Rev. D **22**, 2157 (1980); *Perturbative Quantum Chromodynamics*, edited by A. H. Mueller (World Scientific, Singapore 1989), p. 93; S. J. Brodsky, in Proceedings of the Quantum Chromodynamics Workshop, La Jolla, California, 1978.
- [72] A. V. Efremov and A. V. Radyushkin, Phys. Lett. **94B**, 245 (1980); Theor. Math. Phys. **42**, 97 (1980).
- [73] A. V. Radyushkin, arXiv:hep-ph/0410276.
- [74] A. Duncan and A. H. Mueller, Phys. Rev. D **21**, 1636 (1980).
- [75] S. V. Mikhailov and A. V. Radyushkin, JETP Lett. **43**, 712 (1986); Sov. J. Nucl. Phys. **49**, 494 (1989); Phys. Rev. D **45**, 1754 (1992).
- [76] A. P. Bakulev and A. V. Radyushkin, Phys. Lett. B **271**, 223 (1991).
- [77] A. P. Bakulev and S. V. Mikhailov, Z. Phys. C **68**, 451 (1995).
- [78] B. L. Ioffe and A. V. Smilga, Phys. Lett. **114B**, 353 (1982).
- [79] N. Isgur and C. H. Llewellyn Smith, Phys. Rev. Lett. **52**, 1080 (1984); Nucl. Phys. **B317**, 526 (1989); Phys. Lett. B **217**, 535 (1989).
- [80] A. V. Radyushkin, Acta Phys. Pol. B **15**, 403 (1984); Nucl. Phys. **A527**, 153 (1991); **A532**, 141 (1991).
- [81] O. C. Jacob and L. S. Kisslinger, Phys. Rev. Lett. **56**, 225 (1986).
- [82] R. Jacob and P. Kroll, Phys. Lett. B **315**, 463 (1993).
- [83] J. Bolz *et al.*, Z. Phys. C **66**, 267 (1995).
- [84] V. M. Braun and I. Halperin, Phys. Lett. B **328**, 457 (1994).
- [85] B. Chibisov and A. R. Zhitnitsky, Phys. Rev. D **52**, 5273 (1995).
- [86] D. Melikhov, Phys. Rev. D **53**, 2460 (1996); Eur. Phys. J. direct C **4**, 1 (2002).
- [87] S. Descotes and C. T. Sachrajda, Nucl. Phys. **B625**, 239 (2002).
- [88] S. J. Brodsky, G. P. Lepage, and T. Huang, in *Proceedings of the Banff Summer Institute on Particles and Fields, 1981*, edited by A. Z. Capri and A. N. Kamal (Plenum Press, New York, 1983), p. 143.
- [89] M. A. Shifman, A. I. Vainshtein, and V. I. Zakharov, Nucl. Phys. **B147**, 385 (1979).
- [90] D. V. Shirkov and I. L. Solovtsov, Phys. Rev. Lett. **79**, 1209 (1997); Phys. Lett. B **442**, 344 (1998); Theor. Math. Phys. **120**, 1220 (1999).
- [91] N. G. Stefanis, W. Schroers, and H.-Ch. Kim, Phys. Lett. B **449**, 299 (1999).
- [92] H.-N. Li, Phys. Rev. D **52**, 3958 (1995).
- [93] M. Beneke and Th. Feldmann, Nucl. Phys. **B592**, 3 (2001).
- [94] Z. T. Wei and M. Z. Yang, Nucl. Phys. **B642**, 263 (2002).
- [95] T. Kurimoto, H.-N. Li, and A. I. Sanda, Phys. Rev. D **65**, 014007 (2001).
- [96] H.-N. Li, Phys. Rev. D **66**, 094010 (2002).